AN ABSTRACT OF THE THESIS OF

DONG XIAO for the degree MASTER OF SCIENCE

in PHYSICS presented on June 17, 1985.

Title: GAMMA DECAYS AND LEVEL STRUCTURE OF ^{186}Ir

Abstract Approved: Redacted for Privacy

Dr. Kenneth S. Krane

^{186}Ir gamma transitions are studied via the reaction Hf(^{14}N, xn)Au at ^{14}N beam energy 130 MeV. The beta decay chain of Au is Au → Pt → Ir → Os. Singles and coincidence data are from measurements by Ge gamma-ray detectors. Conversion electrons are measured by Si(Li) detector. The energy and intensity of all the gamma rays are analyzed. The energy uncertainties are less than 0.1 keV. Multipolarities of some gamma transitions are found from conversion electron spectrum. Those gamma transitions from ^{186}Ir excited states are identified. There are so many gamma peaks in the spectrum grouping together that maybe there are still more gamma transitions from ^{186}Ir that are hidden. The gamma transitions of ^{186}Ir presented here add more information to the previous results.

Gamma Decays and Level Structure of ^{186}Ir

by

Dong Xiao

A THESIS

submitted to

Oregon State University

in partial fulfillment of

the requirements for the

degree of

Master of Science

Completed June 17, 1985

Commencement June 1986

APPROVED:

Redacted for Privacy

Professor of Physics in charge of major

Redacted for Privacy

Chairman of Department of Physics

Redacted for Privacy

Dean of Graduate School

Date thesis is presented June 17, 1985

Typed by Kathy Haag for Dong Xiao

ACKNOWLEDGMENTS

My most sincere gratefulness and appreciation is to: Dr. Kenneth S. Krane, for his encouraging and helpful directions and support throughout the work. Dr. Wayne L. Swenson and Dr. Rubin H. Landau, for their helpful discussions of some theoretical questions; also Dr. Rubin H. Landau and Dr. Victor A. Madsen, for allowing me to do the data analysis on their computer; and graduate students Milton E. Sagen and Jeffrey Schnick, for their help on the operation of the computer; Miss Kathy Haag, for her skillful typing work.

TABLE OF CONTENTS

LIST OF FIGURES

LIST OF TABLES

GAMMA DECAYS AND LEVEL STRUCTURE of ^{186}Ir

I. Introduction

There are many efforts being made in studying collective structures in transitional odd-odd nuclei. In the slightly oblate-deformed region below the closed double shell nucleus ^{208}Pb, the nuclear shape changes from oblate to prolate down to the center of the well prolate-deformed rare earth region. Our interest is based on the speculation of the "double decoupling" phenomenon which is probably occurring in the level structure of ^{186}Ir in this transitional region.

In the collective model of odd-odd nuclei, the usual assumption is to consider a single proton and a neutron moving in a deformed even-even core field. Furthermore, we assume a strong coupling model for which the motion of the odd nucleons in the potential formed by the core and seen from the reference frame fixed in the nucleus is identical with that of the nucleons moving in a similar, but spatially fixed, potential. The Hamiltonian of this collective model can be written as

$$H = H_r + H_n + H_p + V_{pn} \qquad (1)$$

where H_p and H_n describe the single-particle motion of the unpaired proton and neutron in the deformed even-even nucleus core field,

$$H_p = \frac{\vec{p}^2}{2m_p} + V_p \ ,$$

$$H_n = \frac{\vec{p}^2}{2m_n} + V_n \ ,$$

and H_r is the rotational energy of the even-even core

$$H_r = \frac{\hbar^2}{2}\left(\frac{L_1^2}{T_1} + \frac{L_2^2}{T_2} + \frac{L_3^2}{T_3}\right) \ ;$$

where L_i (i=1,2,3) are angular momentum components of the deformed core and T_i (i=1,2,3) are moments of inertia: V_{pn} expresses the interaction between the neutron and proton which we will neglect in the following argument for simplicity although it may be significant after all.

Define $\vec{I}$ the total angular momentum, $\vec{L}$ the angular momentum of the even-even core and $\vec{j}_p$ and $\vec{j}_n$ the angular momenta of the odd proton and neutron. Because of deformation, none of these last three are constants of motion but $\vec{I}$:

$$\vec{I} = \vec{L} + \vec{j}_p + \vec{j}_n \ . \qquad (2)$$

The requirement of strong coupling along with the independence of neutron and proton motion implies that [APPENDIX A]

$$\begin{aligned} [I_1, I_2] &= -i\hbar I_3 \quad \text{cyclically}, \\ [j_{p_1}, j_{p_2}] &= i\hbar j_{p_3} \quad \text{cyclically}, \\ [j_{n_1}, j_{n_2}] &= i\hbar j_{n_3} \quad \text{cyclically}, \end{aligned} \qquad (3)$$

and

$$[\vec{j}_p, \vec{j}_n] = 0.$$

The projection of $\vec{I}$ upon the laboratory Z-axis is M: its projection on the body-fixed 3-axis is taken as K and the projections of $\vec{j}_p$ and $\vec{j}_n$ are taken as Ω_p and Ω_n. $\vec{I}^2$ and I_z will be constants of motion. If we assume the system is symmetric along the 3-axis, Ω_p, Ω_n, and K will be constants of motion, too. (Fig. 1)

Assume the nucleus as well as the deformed core are symmetric about the body-fixed 3-axis and therefore, at least for the ground state rotational band, $L_3=0$: thus Eq. (2) shows that $K = \Omega_p + \Omega_n$. Because of the nuclear symmetry, the particle states are degenerate with respect to the sign of Ω so that, more precisely,

$$K = |\Omega_p \pm \Omega_n| \,. \tag{4}$$

Applying the axial symmetry condition $T_1=T_2=T_0$ and using Eq. (2), we can rewrite the Hamiltonian as

$$H = H_R + H_{p,n} + H_c \tag{5}$$

where

$$H_R = A\,[I(I+1) - K^2] \tag{6}$$

$$H_{p,n} = \frac{\vec{P}^2}{2m_p} + V_p + A\,(j_{p_1}^2 + j_{p_2}^2) + \frac{\vec{P}^2}{2m_n} + V_n + A\,(j_{n_1}^2 + j_{n_2}^2)$$

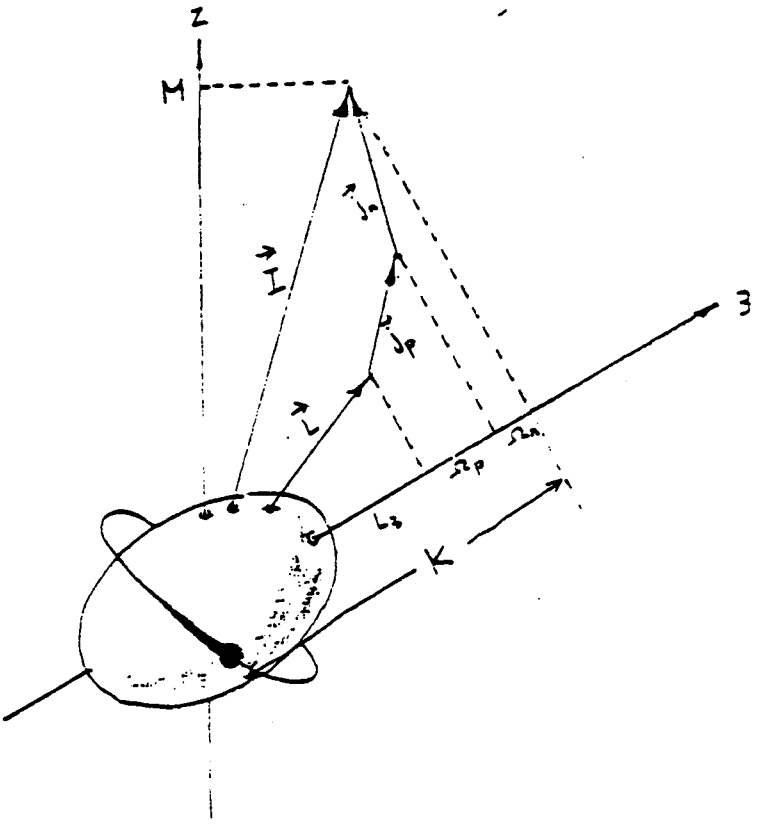

Fig. 1 The collective model of odd-odd nucleus. The projection of the total angular momentum $\vec{I}$ of an odd-odd nucleus on the laboratory Z-axis (M) and on the body-fixed 3-axis (K). The quantum numbers Ω_p, Ω_n are the projections of two odd nucleons angular momenta j_p, j_n on the 3-axis. When $L_3=0$, $K=\Omega_p \pm \Omega_n$.

$$H_c = -2A\left[(I_1 j_{p_1} + I_2 j_{p_2}) + (I_1 j_{n_1} + I_2 j_{n_2}) - (j_{p_1} j_{n_1} + j_{p_2} j_{n_2})\right] \qquad (8)$$

with

$$A = \frac{\hbar^2}{2T_0} .$$

The last term is classically the Coriolis force so that it will be called the Coriolis term. It is this term that causes the decoupling of the nucleons with the rotational band. We will see its effect later. For now, except for the special case where H_c has diagonal contributions, we can neglect its effect and the rotational and particle equations separate

$$|^{186}I_r\rangle = |EIMK\rangle|\Omega\rangle \qquad (9)$$

where $|EIMK\rangle$ is the rotational function which is associated with the eigenvalue problem

$$H_R|EIMK\rangle = A[I(I+1)-K^2]|EIMK\rangle \qquad (10)$$

and $|\Omega\rangle$ is the particle function which is the solution of

$$H_{p,n}|\Omega\rangle = (E_p + E_n)|\Omega\rangle = E_{p,n}|\Omega\rangle \qquad (11)$$

The Schroedinger equation becomes

$$H|EIMK=\Omega_p+\Omega_n\rangle = [H_R|EIMK\rangle|\Omega\rangle + |EIMK\rangle H_{p,n}|\Omega\rangle]$$

$$= E_{I,K}\,|\,EIMK=\Omega_p+\Omega_n\rangle \qquad (12)$$

Now we can see how the odd particles couple together to form the K band. From

$$E_{I,K} = A\,[I(I+1) - K^2] + E_p + E_n \qquad (13)$$

it is obvious that the rotational bands start from I=K ($K=\Omega_p+\Omega_n$ or $K=|\Omega_p-\Omega_n|$); a pair of particles will form two rotational bands of the form

$$I_1 = |\Omega_p-\Omega_n|,\ |\Omega_p-\Omega_n|+1,\ |\Omega_p-\Omega_n|+2,\ \cdots$$

$$I_2 = \Omega_p+\Omega_n,\ \Omega_p+\Omega_n+1,\ \Omega_p+\Omega_n+2,\ \cdots \qquad (14)$$

and with heads at

$$E_{I,K_1} = A\,|\Omega_p-\Omega_n| + E_p + E_n$$

$$E_{I,K_2} = A\,(\Omega_p+\Omega_n) + E_p + E_n\,. \qquad (15)$$

The question now is which of the two bands contains the ground state. The ground state band is determined by a set of empirical rules assuming the intrinsic spins of the odd proton and neutron S_p and S_n ($\Omega_p=S_p+\ell_p$, $\Omega_n=S_n+\ell_n$) are always parallel coupled. From this assumption we obtain the coupling rules [1], [2]

$$I_0 = |\Omega_p - \Omega_n| \; ; \quad \text{if } \Omega_p = l_p \pm \tfrac{1}{2}, \; \Omega_n = l_n \mp \tfrac{1}{2}$$

$$I_0 = \Omega_p + \Omega_n \; ; \quad \text{if } \Omega_p = l_p \pm \tfrac{1}{2}, \; \Omega_n = l_n \pm \tfrac{1}{2}. \qquad (16)$$

It has been shown that these rules account in general for the ground state spins of deformed odd-odd nuclei.

In order to solve the level structure problem, we have to consider the matrix elements of H_c.

By defining the raising and lowering operators

$$\begin{cases} a^+ = a_1 + i a_2 \\ a^- = a_1 - i a_2 \end{cases} \qquad (17)$$

the Coriolis term H_c becomes

$$H_c = -A\left[(I^+ j_p^- + I^- j_p^+) + (I^+ j_n^- + I^- j_n^+) - (j_p^- j_n^+ + j_p^+ j_n^-)\right]. \qquad (18)$$

The last two terms make diagonal contributions whereas the others usually have only zero diagonal matrix elements. As we will see, the diagonal contribution arises only when the two nucleons in $\Omega=1/2$ bands couple to $K=0$ because the nucleus has axial symmetry, i.e. the wave function has to be symmetric for K and -K.

So, in order to calculate the matrix elements of H_c the state function needs to be symmetrized. The symetrization procedure is shown in APPENDIX B where we use the coupled particle representation.

$$|\Omega\rangle = \sum_j C_{j\Omega} |j\,\Omega\rangle \qquad (19)$$

The symmetrized state functions are represented by

$$\left| EIMK = |\Omega_p \pm \Omega_n| \right\rangle . \qquad (20)$$

By going through some algebra, finally we can get the diagonal elements of H_c as

$$\langle EIMK=0| H_c | EIMK=0 \rangle = \frac{\hbar^2}{2T_0} (-1)^{I+1}$$

$$\times a_p a_n \delta_{K,0} \left(\delta_{\Omega_p,\frac{1}{2}} \delta_{\Omega_n,-\frac{1}{2}} + \delta_{\Omega_p,-\frac{1}{2}} \delta_{\Omega_n,\frac{1}{2}} \right), \qquad (21)$$

where a_p and a_n are, respectively, the proton and neutron decoupling parameters

$$a = \sum_j (-1)^{j+\frac{1}{2}} \left(j+\tfrac{1}{2}\right) \left| C_{j,\frac{1}{2}} \right|^2 . \qquad (22)$$

Adding these diagonal contributions to the eigenvalue expression (13) yields

$$E_{I,K} = \frac{\hbar^2}{2T_0} \left[I(I+1) - K^2 + \right.$$

$$\left. (-1)^{I+1} a_p a_n \delta_{K,0} \left(\delta_{\Omega_p,\frac{1}{2}} \delta_{\Omega_n,-\frac{1}{2}} + \delta_{\Omega_p,-\frac{1}{2}} \delta_{\Omega_n,\frac{1}{2}} \right) \right]$$

$$+ E_p + E_n . \qquad (23)$$

It should be noted in this expression that for the K=0 bands, the last term in the brackets alternates in sign which will provide displacement of even spin and odd

spin rotational levels for this K=0 band. For this case there will be coupling by H_c to the K=1 bands that are formed by the opposite coupling of the Ω=1/2 particle states.

It should be kept in mind that H_c also has off-diagonal contributions $\langle EIMK=1|H_c|EIMK=0\rangle$, which we will discuss later in the decoupling procedure.

An example of odd-odd deformed nuclei is ^{186}Ir. Fig. 2 shows the level scheme of ^{186}Ir proposed recently by Kreiner et al. [3] with rotational band of an even-even nucleus ^{184}Os. It appears to have a normal rotational band as compared with ^{184}Os except its spin starts from 5 which causes questioning.

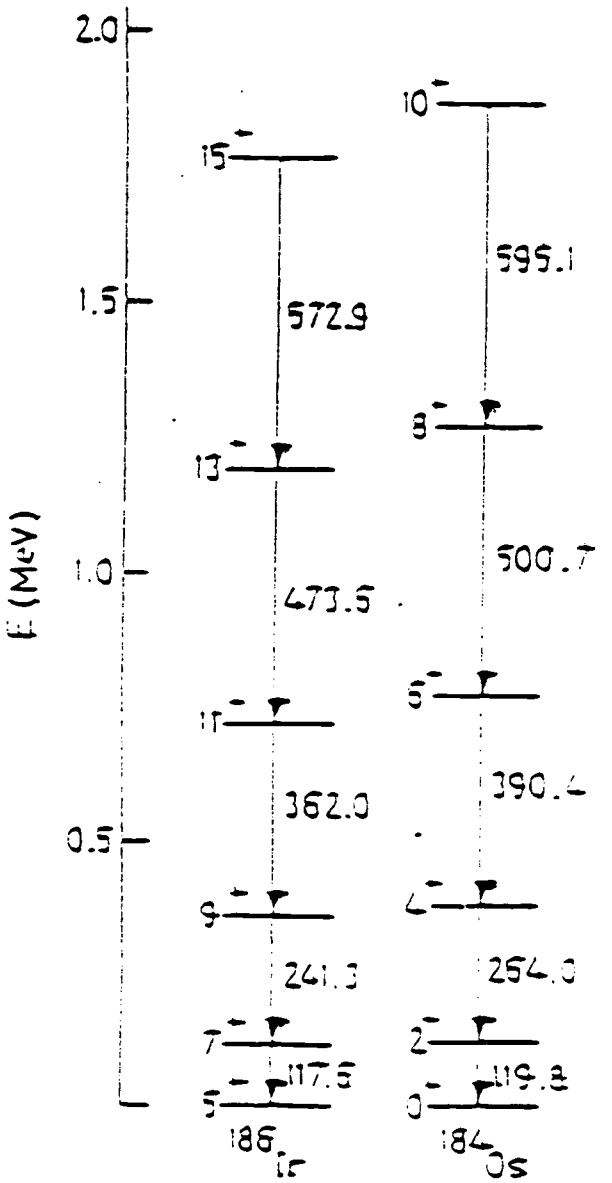

Fig. 2 The rotational band of 5^+ state in ^{186}Ir compared with ^{184}Os ground gand. (From Kreiner et al. Nucl. Phys. A432, 451, 1985)

II. ^{186}Ir level structure

The ^{186}Ir ground state has been studied for years to understand its collective properties. It is in a transitional region below Pb where the $\pi(h9/2)*\nu(i13/2)$ semidecoupled two-quasiparticle structure was identified [4],[5]. One of the facts concerning the odd-odd nuclear state is that the spin-parity assignment alone is usually not enough for identification because several possible orbits of two single quasiparticles can couple with each other to the same spin-parity state. So another quantum number K is being used for naming a state.

There are two known isomeric states in ^{186}Ir. They are $I^{\pi}=2^{-}$, T =1.7hr and $I^{\pi}=5^{+}$, T =15.8hr. Both are observed in the present work. It was proposed that the ^{186}Ir ground state has total angular momentum I=5 and its projection on the body-fixed reference frame K=0,1. The arguments are based on beta-decay properties, atomic beam experiment, and the measurements of its magnetic dipole moment and electric quadrupole moment.

1. Atomic beam experiments.

By atomic beam magnetic resonance method, Rubinsztein and Gustafsson [6] confirmed that I=5 for 15.8hr ^{186}Ir ground state. Their configuration assignment was proton 1/2[541], neutron 1/2[510]. They also got I=5/2 for ^{185}Ir

ground state rather than 3/2 for other heavier odd-A iridium isotopes.

2. Beta-decay studies.

Experiments (Spanhoff et al. [8], Hoffstetter et al. [7]) showed that the ^{186}Ir β-decay to ^{186}Os daughter states only populates spin 4, 5 or 6 and almost only on even states (with log ft values in the range of 7-8 which is corresponding to ΔK=0 or 1). Moreover, the majority of the beta intensity populates ^{186}Os states with low spin projection K, primarily K=0 (ground state and beta vibrational) and K=2 (gamma vibrational) bands. By those evidences, Hofstetter et al. [7] suggested $I^{\pi}K=5^{+}1$ as the coupling of a proton in a $1/2^{-}[541]$ Nilsson state and a neutron in a $1/2^{-}[510]$ state.

3. Nuclear magnetic moment of ^{186}Ir.

Measurements of static quadrupole and magnetic dipole moments were performed to further investigate the structure of the ground state. There have been several groups studying the nuclear magnetic moment of ^{186}Ir. Spanhoff et al. in 1978 reported their experimental value $\mu=2.8(3)\,\mu_N$.[8] They found that this value would be contradictory with a $I^{\pi}K=5^{+}1$ configuration. But Hagn and Zech in 1980 [9] reported $\mu=3.80^{+0.12}_{-0.02}\,\mu_N$ and gave an explanation in terms of mixed ground state configuration of K=0 and 1. Dr. Krane and his Oxford collaborators

confirmed Hagn and Zech's results with $\mu=3.88(5)\mu_N$. [10]

The magnetic moment is given by

$$\mu = g_R I + (g_K - g_R)\frac{K^2}{I+1} \qquad (24)$$

where g_R and g_K are the rotational and intrinsic g factors respectively. Generally, $g_K \approx 1$, $g_R \approx Z/A$ and in our case $g_R \approx 0.41$, so that one expects $\mu \approx 2.1\text{-}2.2\mu_N$ for K=0 or 1. This is inconsistent with the measured value of $3.9\mu_N$. But if we assume that there is band mixing between K=0 and K=1 bands, the value 3.9 will come out naturally. Or in other words, instead of incoherent superposition of the moments of the individual pure-K states:

$$\mu = A^2\mu(K_1) + B^2\mu(K_2) \qquad (25)$$

we consider the interference term AB playing an important role.

The possible coupling in terms of proton and neutron Nilsson orbits is $1/2^-[541]_p + 1/2^-[510]_n$. The wave-function will be

$$|^{186}I_r\rangle = A|EIMK=0\rangle + B|EIMK=1\rangle \qquad (26)$$

with $A^2+B^2=1$. The rotational wavefunctions $|EIMK=\Omega\rangle$ are shown in APPENDIX B. Following some straightforward calculations and arguments [10], the magnetic moment of this mixed configuration is found to be

$$\mu = 2.05 - 0.12B^2 - 4.88AB \qquad (27)$$

The experimental value of $\mu=3.9\mu_N$ requires $A^2=0.8$, $B^2=0.2$ or else $A^2=0.2$ and $B^2=0.8$.

This is a strong evidence of the presence of mixing bands in ^{186}Ir due to the Coriolis coupling.

4. The nuclear electric quadrupole moment of ^{186}Ir.

I and K assignments for the ground state can be confirmed by the measurement of the electric quadrupole moment by applying the Bohr-Mottelson formula

$$Q = Q_0 \frac{3K^2 - I(I+1)}{(I+1)(2I+3)} \qquad (28)$$

where Q_0 is the intrinsic quadrupole moment, which is fixed by deformation parameters in the rotational model. Hagn and Zech found that Q=-3.00(15)b [9]. This Q value together with a I=5 and mixing K=0 or K=1 configuration is consistent with reasonable Q_0-values in this mass region.

It has been a puzzle concerning the I and K quantum numbers for the ground state of ^{186}Ir because usually the level structure of rotational bands is that with sequence

$I=K,K+1,K+2,\ldots$, built on the particle levels $E_{p,n}$. But in this case, the quantum number I started from 5 whereas K=0 or 1. This is presumably due to the double-decoupling phenomena in analogy with decoupling in odd-A nuclei where the ordering inversions in the K=1/2 rotational bands are often seen. Take an odd-A rotational band, for example; the level energies with K=1/2 are given by

$$E = I(I+1) - (-1)^{I+1} |a| (I+\tfrac{1}{2}) \qquad (29)$$

where E is in the unit of rotational constant $A=h^2/8\pi^2T_o$. The second term is the diagonal contribution of H_c, which is linear in angular momentum and is signature dependent. $(-1)^{I+1/2}$ splits the band into two parts by raising the odd I+1/2 levels and lowering the even I+1/2 levels. With

$$E \approx I^2 - |a| I \qquad (30)$$

the lowest energy turns out to be $E_{min} = -a^2/4$ at $I_{min} = |a|/2$. So, for different values of a, we can get different spin for the lowest level (Fig. 3a). Fig. 4 shows an example of odd-A nucleus (^{237}Np) levels where some of the higher spin levels come down below their band head. The negative Coriolis term decouples the "valence" nucleon from the rotational band for a critical value $|a| \geq 1$.

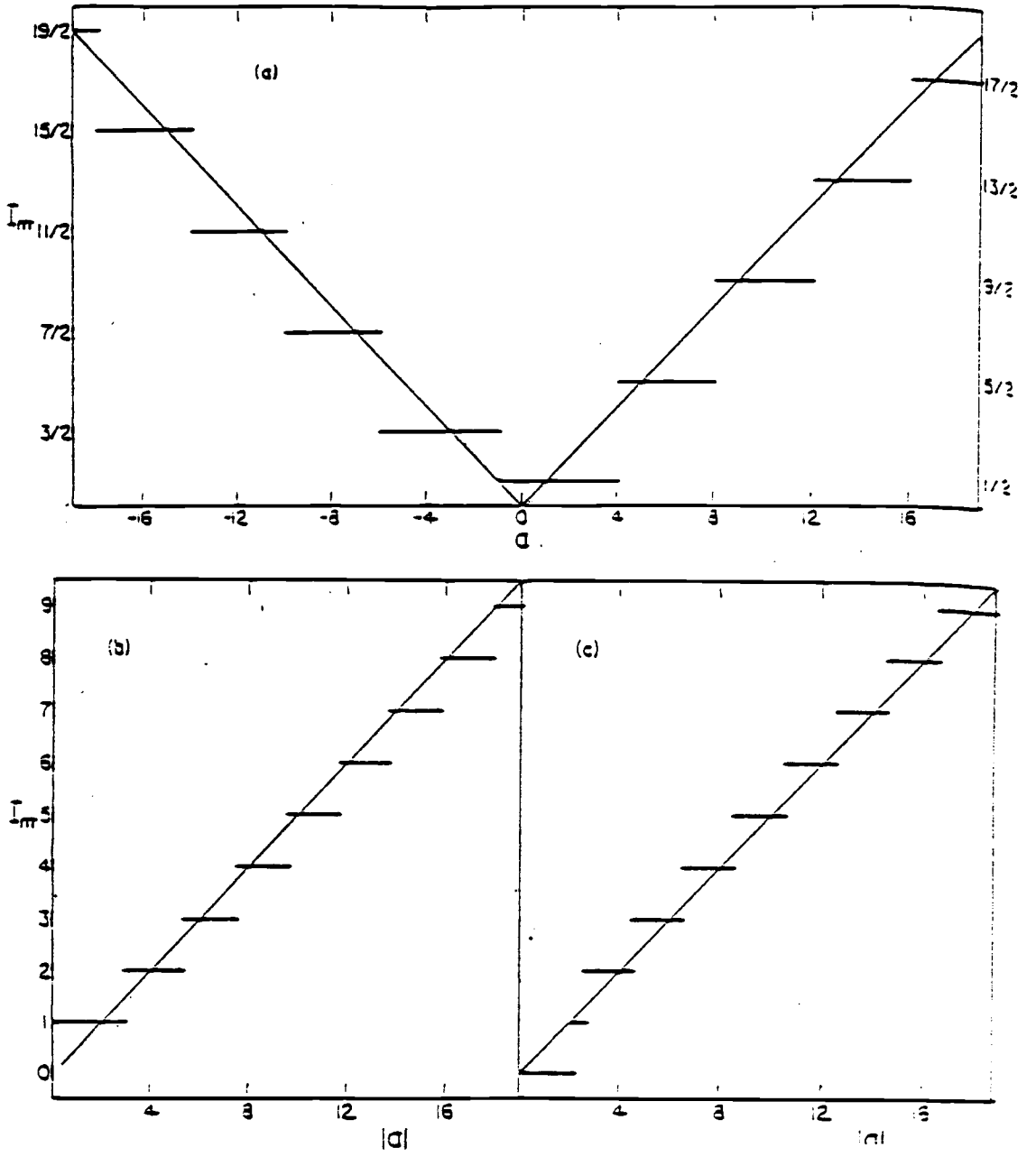

Fig. 3 Angular momentum I_{min} of the lowest level as a function of the decoupling parameter a. (a) Odd-A nucleus with K=1/2 band. (b) Two-quasiparticle system with K=1,2 (Ω_1=3/2,Ω_2=1/2). (c) Two-quasiparticle system with K=0,1,1,2 (four band coupling)

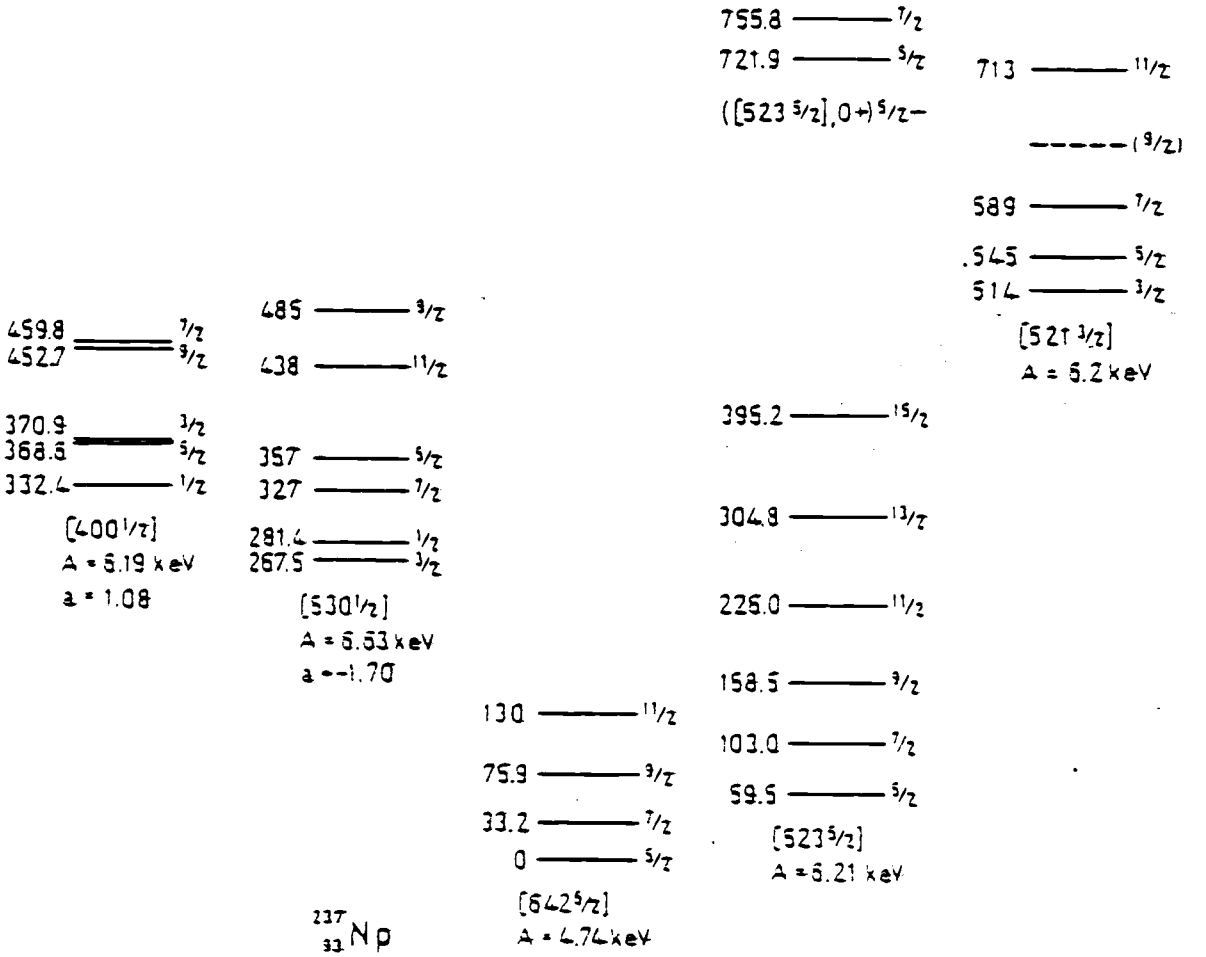

Fig. 4 Level scheme of ^{237}Np. The level scheme is from Bohr and Mottelson "Nuclear Structure". Data is based partly on the decay of ^{241}Am (S. A. Baranov, V. M. Kulakov and V. M. Shatinsky, Nucl. Phys. 56, 252, 1964, and C. M. Lederer, J. K. Poggenburg, F. Asaro, J. O. Rasmussen and I. Perlman, Nucl. Phys. 84, 481, 1966) and partly based on one-particle transfer studies (Th.W. Elze and J. R. Huizenga, Phys. Rev. C1, 328, 1970).

This decoupling effect is a general one. For the two quasi-particle system, the neutron proton "double decoupling" occurs from critical values for both decoupling parameters $|a_n|, |a_p| \geq 1$. In order to understand the decoupling process in this situation, recall that in odd-odd nuclei, the Hamiltonian has a diagonal term $\langle K=0, 1|H_c|K=0,1\rangle$ and an off-diagonal term $\langle K=1|H_c|K=0\rangle$. The diagonal term does not contribute a negative energy in our case; however, the decoupling is related to the off-diagonal matrix element in a way that $K=\Omega_p+\Omega_n=1$ and $K=\Omega_p-\Omega_n=0$ for $\Omega_p=\Omega_n=1/2$. This off-diagonal matrix element comes out to be

$$-A\left(a_p + a_n(-1)^{I+1}\right)\left[I(I+1)\right]^{\frac{1}{2}} \qquad (31)$$

a_p and a_n being the decoupling parameters of proton and neutron and $a=a_p+a_n(-1)^{I+1}$. Then we evaluate the eigenvalue of the secular equation to get the energy correcton [11]. The off-diagonal part contributes a negative signature- and I-dependent energy term. Apparently, I_{min} is still proportional to $|a|$. Generally, the positive diagonal rotational energy is proportional to the square of the angular momentum, and the negative off-diagonal Coriolis term increases with a lower power of the angular momentum. In the limit where the off-diagonal matrix elements are much larger than the zero-order diag-

onal energy splittings, the negative Coriolis contribution becomes linear in the angular momentum, and we still get $E/A \approx I^2 - |a| I$ with $E_{min} \approx -a^2/4$ at $I_{min} \approx |a|/2$.

A calculation was given by Emery et al. [12]. They have shown that a system involving the $1/2^-[541]$ proton orbital and a low Ω [512] or [510] neutron state would in fact provide a natural explanation for the peculiarity of the ^{186}Ir ground state by calculating the Coriolis matrix element between the proton-neutron coupled states. When the decoupling parameters a_n and a_p are sufficiently large, there will be decoupling which will lower the high I states. [Fig. 5]

To see the level order inversion, $|a_p|$ and $|a_n|$ have to be large compared to 1, so that the lowest energy in the system would occur at a value of I which is larger than the lowest value of I available, i.e. the ordering of the rotational band is reversed. There is a discussion in reference [13] (Fig. 6). In the figure, we can see that the double decoupling occurs at $x_o = a_n/a_p = 1/a_p$ (i.e. $a_n = 1$). This explains quite well the ground state band observed in Fig. 2 where we have a $\Delta I = 2$ band starting with I=5. This band looks like a decoupled sequence where the parity unfavored members, [14] in this case the even spin states, are shifted above the corresponding parity favored states. Besides, in order to have I=5 band as favored,

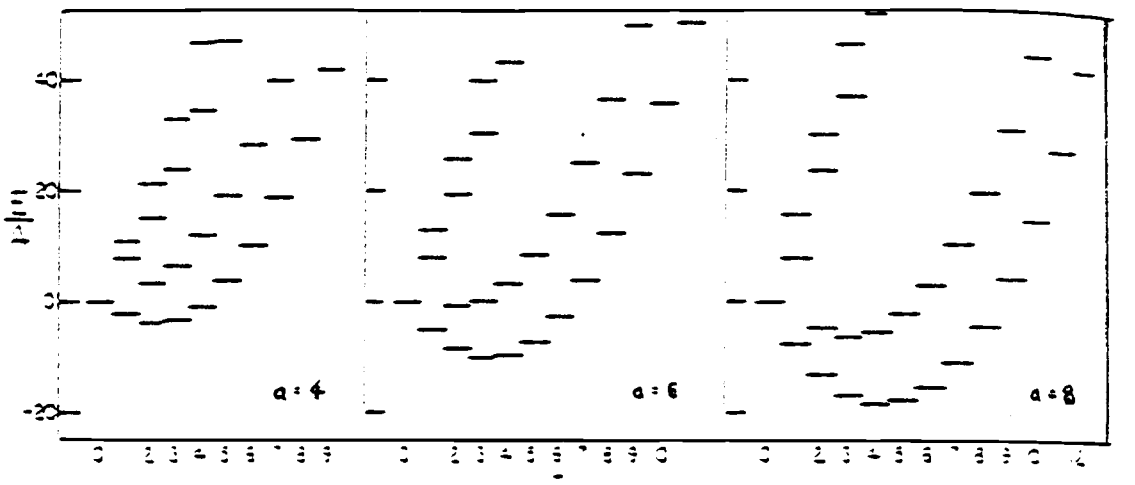

Fig. 5 Energy levels of four-band two-quasiparticle system described in Emergy et al. Nucl. Phys. A211, 189, 1973.

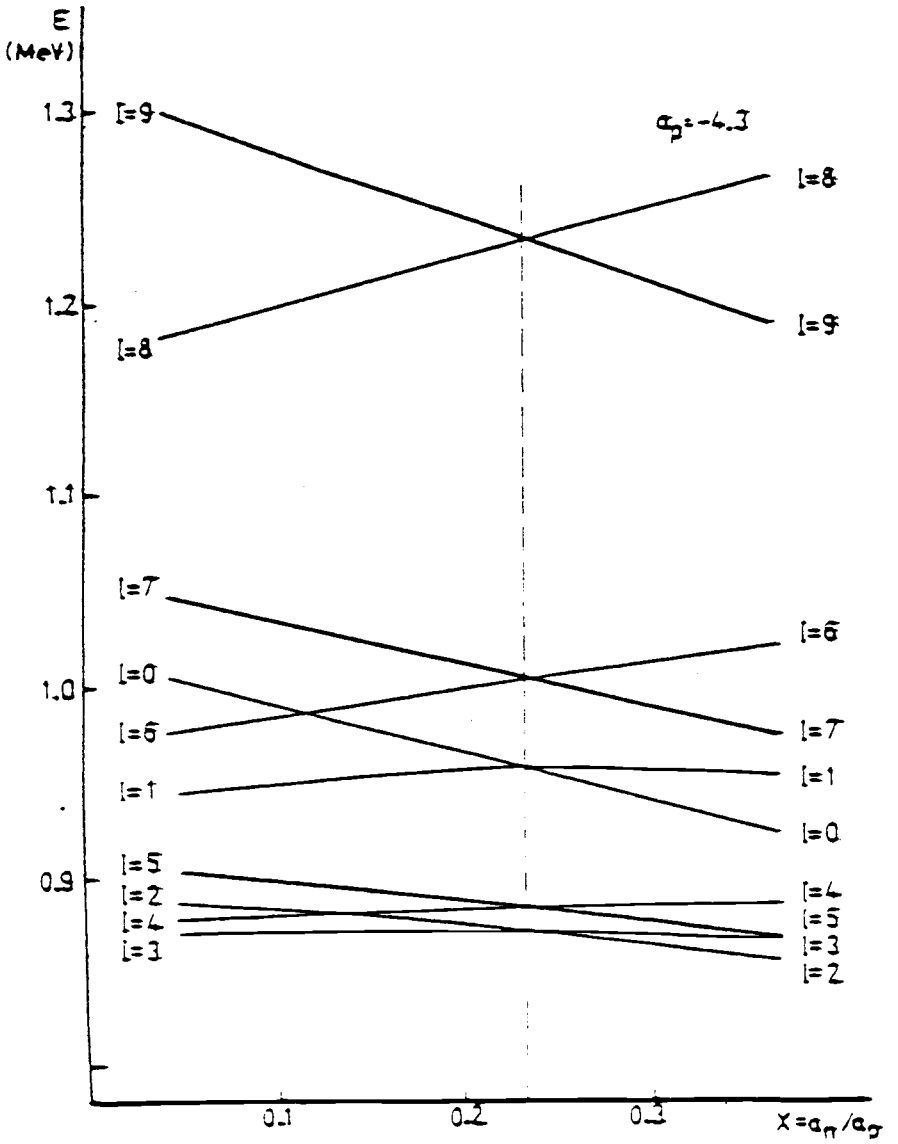

Fig. 6 Excitation energies of odd-odd system as functions of a_n/a_p for $|a_p|$=4.3. The deformation β=0.20.

states, a_n and a_p should have the same sign. This means that the two nucleons are decoupled individually so that this procedure is called double decoupling.

Fig. 7 shows a calculation by Kreiner [13] where all 5 states of $\pi(h_{9/2})$ parentage have been coupled to a single $K=1/2^-$ neutron orbital. The 5^+ state is very close to the ground state and no other available configuration gives similar results. Thus, the evidence on the 5^+ band seems to suggest that, possibly due to the residual proton-neutron interaction V_{pn}, the $h_{9/2}$ proton with $\Omega_p=1/2^+$ and a $i_{13/2}$ neutron with $\Omega_n=1/2^-$ has come down in energy to contribute the major part in the ^{186}Ir ground state band.

Based on all the experimental evidence, the ground state band of ^{186}Ir is possibly the case where such a coupling scheme is realized. Up to now, the level structure of ^{186}Ir is still not completely established.

As we have seen, the study of the ^{186}Ir level scheme would permit direct determination of the inverted ordering and the Coriolis coupling between the K=0 and K=1 bands.

Recently, Kreiner et al. reported a new experiment and proposed a level scheme (Fig. 8). There are two 5^+ bands with $\Delta I=1$ and 2. But there is no information on low-spin states from their results: i.e. the I=0,1,2 members of K=0,1 bands. Our data from the decay of Pt 0^+ ground state should contain this information.

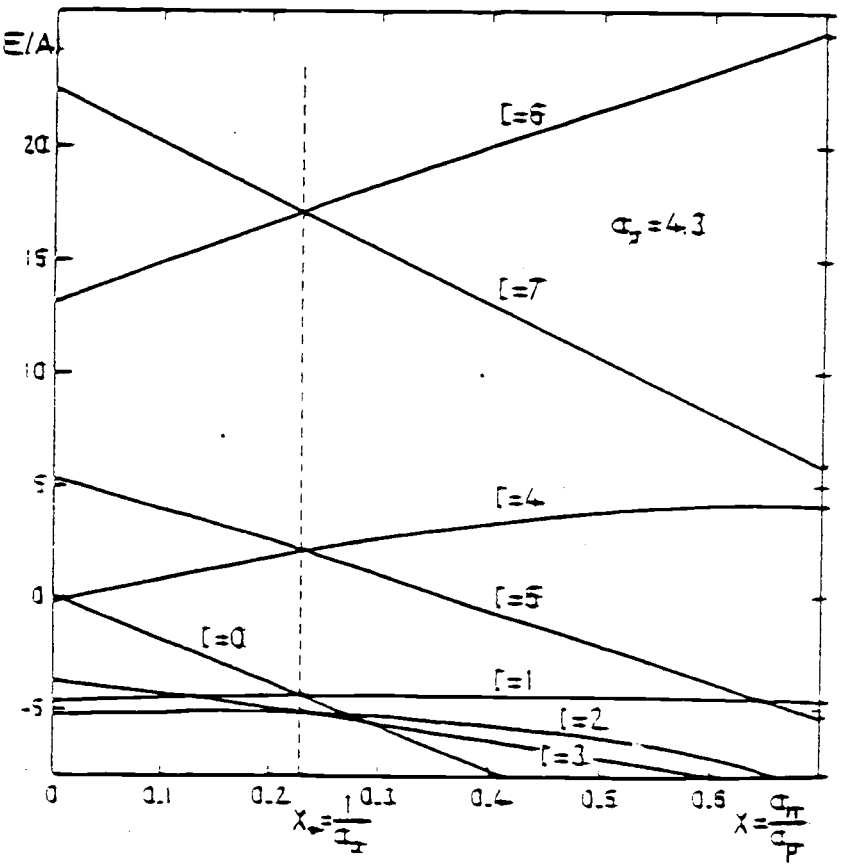

Fig. 7 Energies in units of $A=\hbar^2/2T_0$ as functions of $x=a_n/a_p$ for a two band ($K=1=(1/2)_n+(1/2)_p$, and $K=0=(1/2)_n-(1/2)_p$) Odd-odd system.

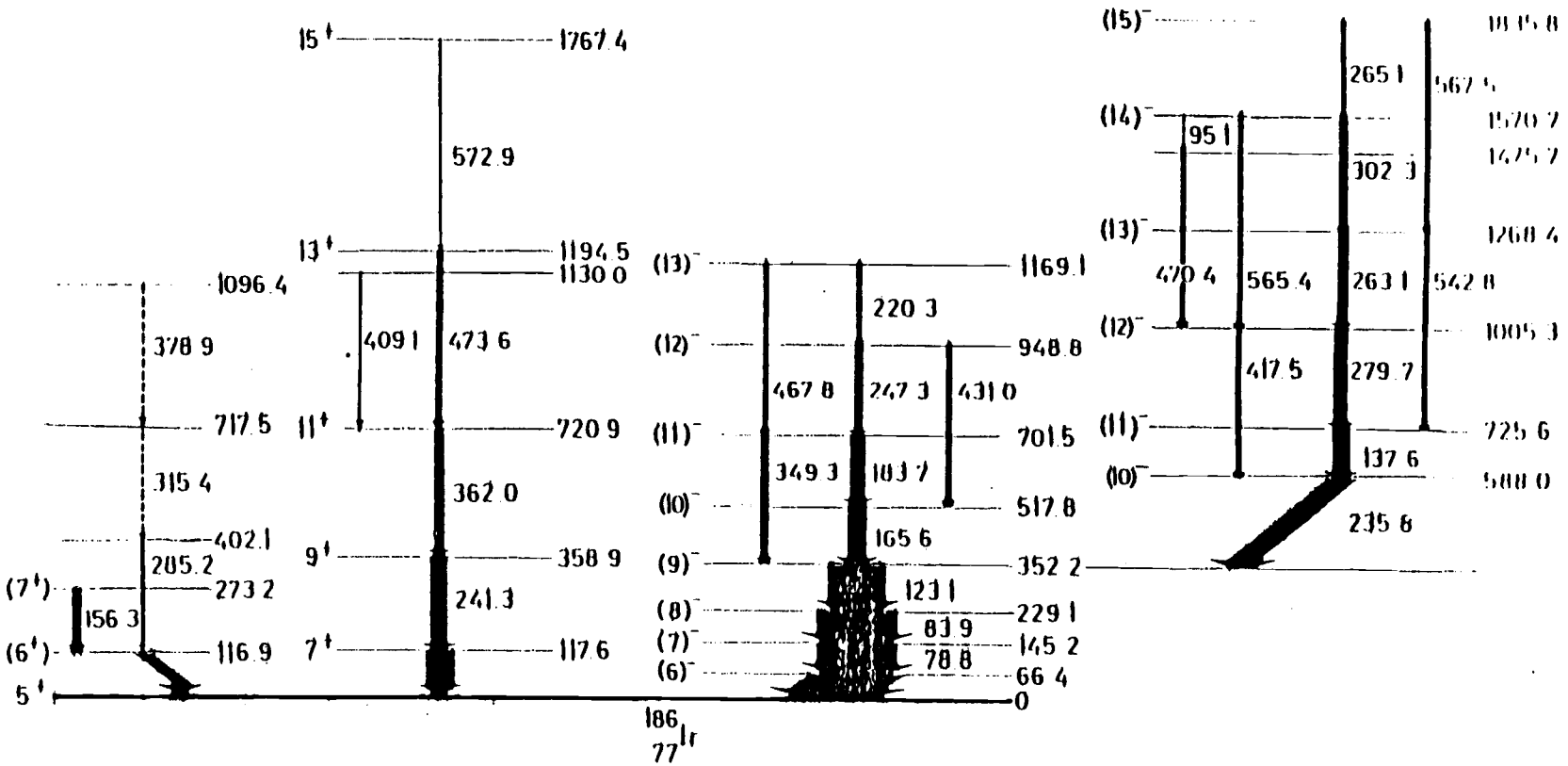

Fig. 8 Level scheme of ^{186}Ir proposed by Kreiner et al. where only the high spin states are presented.

III. Experiment and data analysis

The experiment was performed at the Holifield Heavy Ion Research Facility of the Oak Ridge National Laboratory (ORNL) [Fig. 9]. The radio isotopes ^{184}Ir and ^{186}Ir are produced by using heavy ion beam ^{14}N bombarding on target Hf. The reaction chain is

$$Hf(^{14}N, xn)Au$$

$$Au \longrightarrow Pt + \beta^+$$

$$\hookrightarrow Ir + \beta^+$$

The heavy ion beam available from the Oak Ridge Isochronous Cyclotron (ORIC) was chosen 130 Mev in energy at which both Ir isotopes have about the same cross-section (Fig. 10). Then the beam was directed to the UNISOR (University Isotope Separator at Oak Ridge) where the reaction took place; the isotopes were produced and separated (Fig. 11). The target was placed in the box (2), which was a thin foil (a few mg/cm^2) of natural Hf. The target thickness was chosen so that all reaction products can recoil out of the target material. The product Au nuclei then went through an isotope separator having a 90° deflection and 1.5m radius-of-curvature. The mass resolution is $\delta m/m < 1/2000$ and a mass range of ±8% is accommodated within the collection chamber. Then the isotopes were

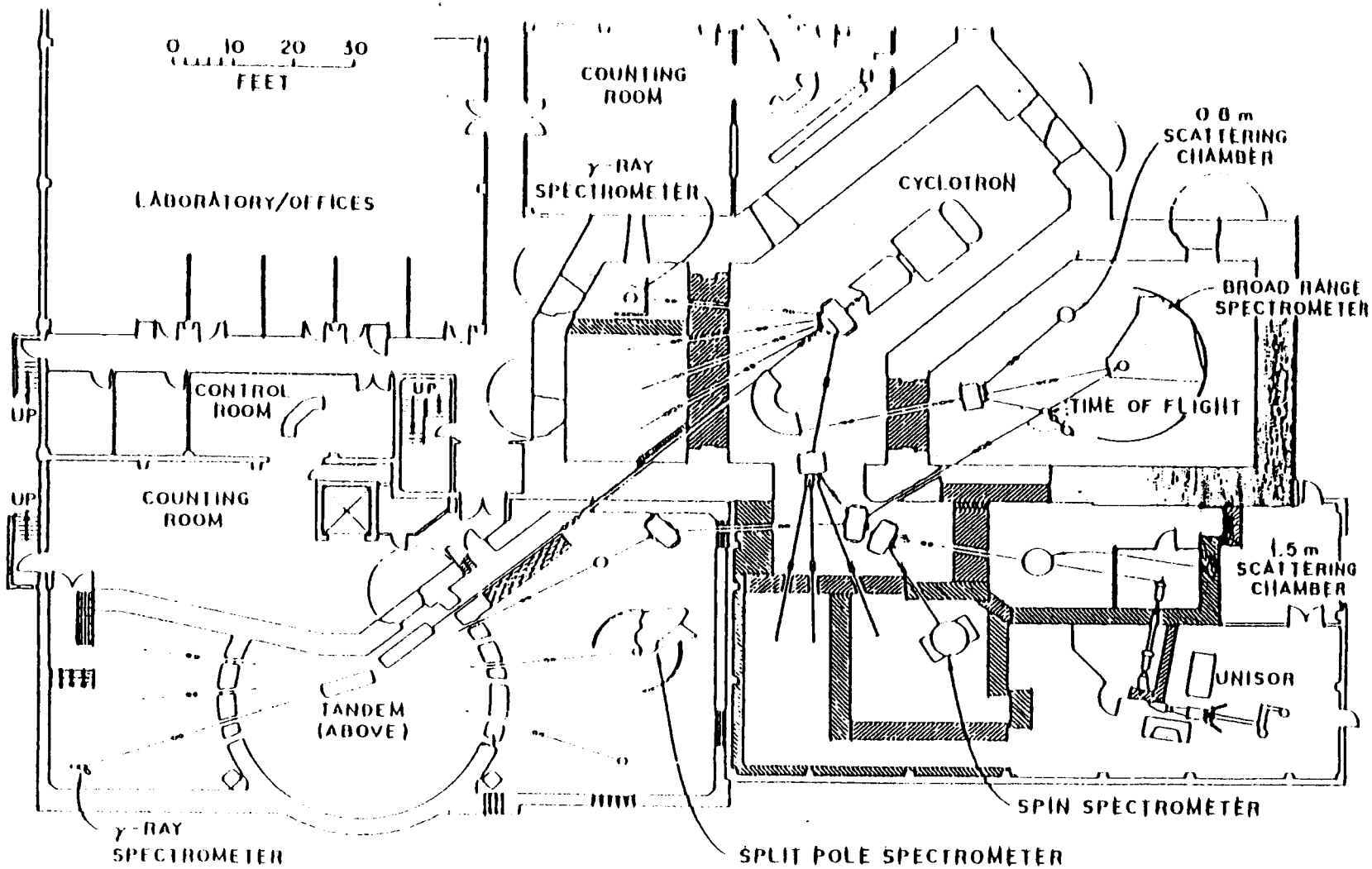

Fig. 9 Holifield Heavy-Ion Research Facility at Oak Ridge National Laboratory. The UNISOR facility is on the lower right.

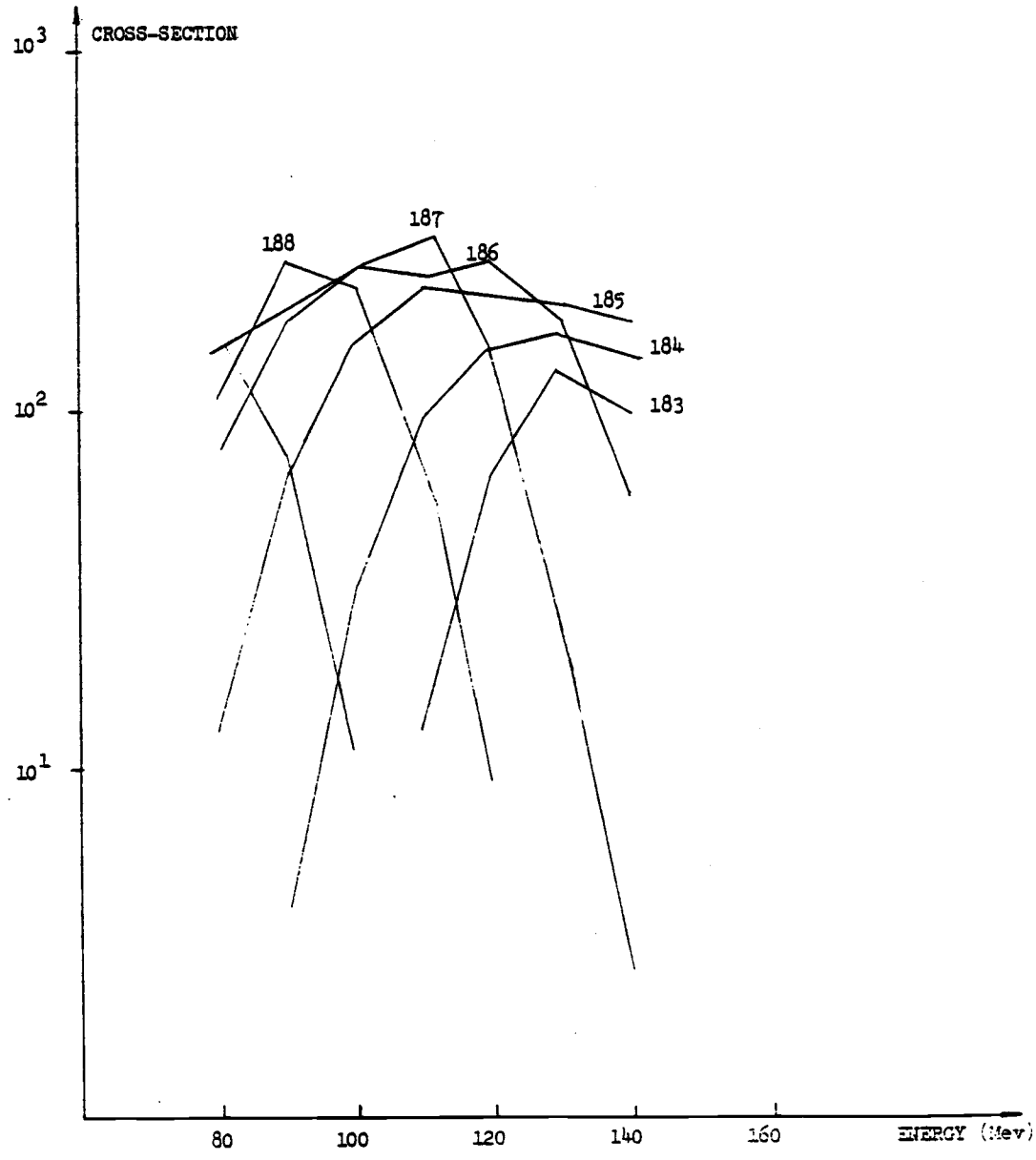

Fig. 10 Cross-sections of Ir isotope production as function of energy.

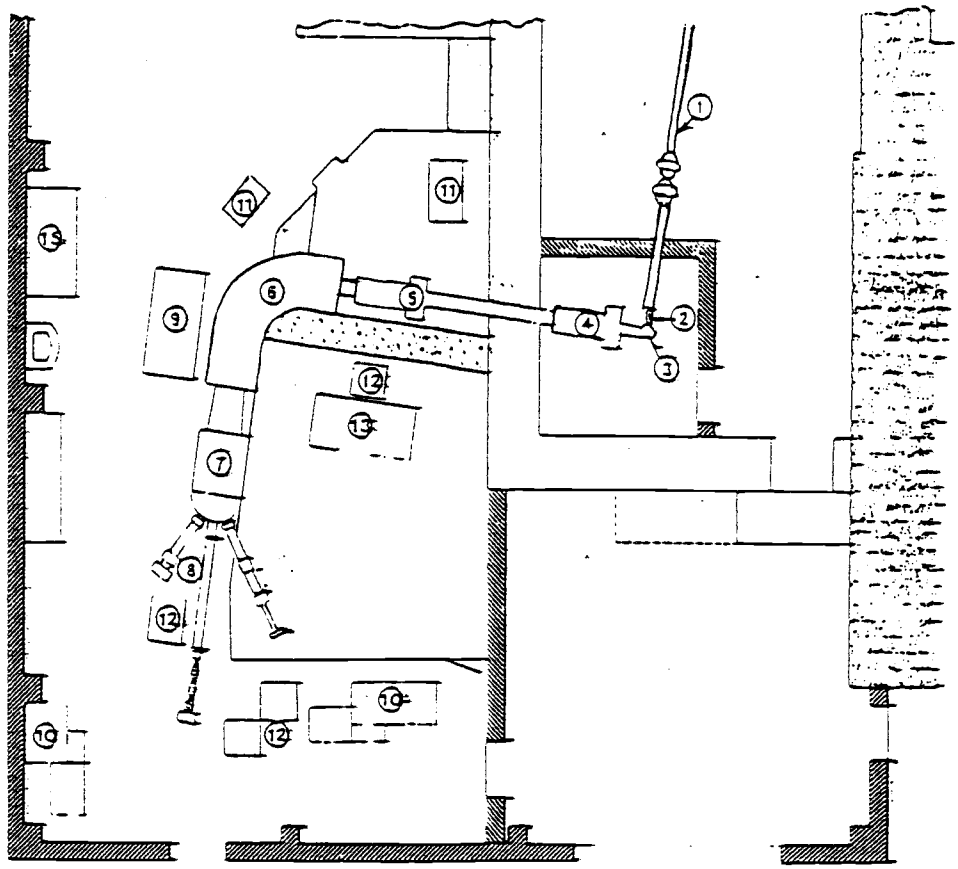

Fig. 11 The UNISOR facility. The major equipment are numbered as follows: (1)beam line;(2)multi-function box, target;(3)on-line ion source position;(4)extractor and lens box;(5)second lens box;(6)dispersion magnet,(7)collection chamber;(8)three separated beam lines;(9)separation control; (10)data-acquisition systems;(11)power supplies;(12)electronics;(13)laser table;(14)laser experiment chamber;(15) chemical hood.

separated into a central line and two deflected lines with angles ±30° (Fig. 12). Two coaxial Ge detectors were placed aside the central ($\gamma\gamma$) line for single and coincidence γ detection. On 30° ($e\gamma$) line there were a Ge detector for γ-rays and a Si(Li) detector for conversion electrons. Fig. 13 shows the configuration of the detectors and the magnetic tape which was used to deposit the radioactive isotopes and transport them to between the detectors.

The data acquisition procedure was as follows:

Configuration #1:

Feed ^{184}Au into $e\gamma$ line and deposit 15 minutes, then let it decay for 3 minutes with the target moved. Then count 24 runs each for 30 seconds. At the same time deposit ^{186}Au onto a focal plane shutter (off-line), collect 90 minutes, decay 30 minutes, then move in between the detectors to count 30 runs with 3 minutes each.

Configuration #2:

Feed ^{186}Au into $e\gamma$ line to collect 90 minutes, decay 30 minutes, count 30 runs for 3 minutes each. And feed ^{184}Au into $\gamma\gamma$ line to collect 15 minutes, decay 3 minutes, then count 24 runs in 30 seconds interval.

All the $\gamma\gamma$ or $e\gamma$ runs were summed up to a grand sum. The $\gamma\gamma$ and $e\gamma$ data were analyzed using a gamma-ray

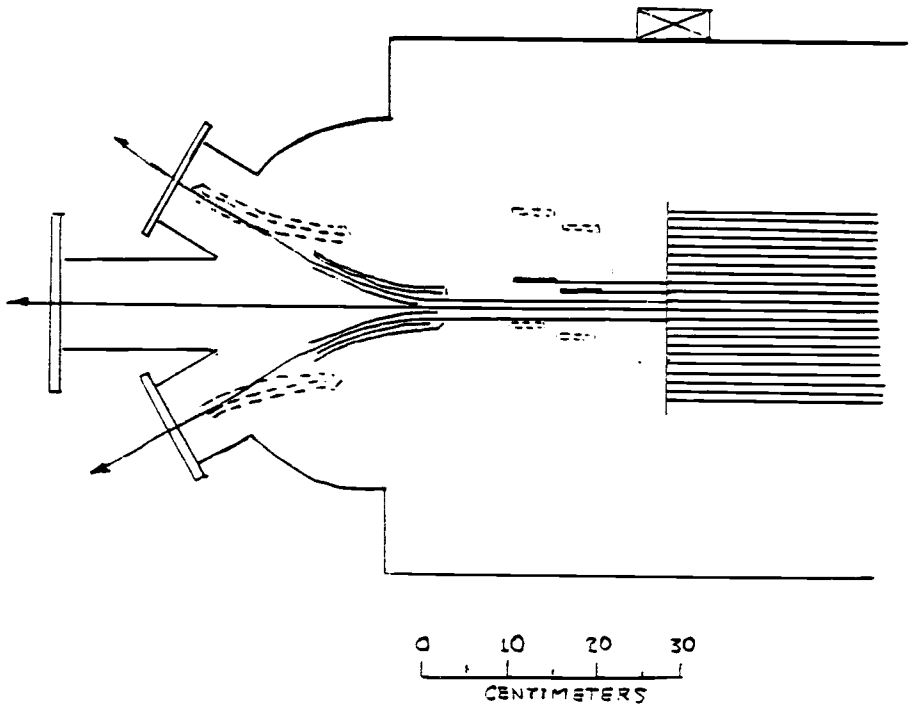

Fig.12. UNISOR isotope separator.

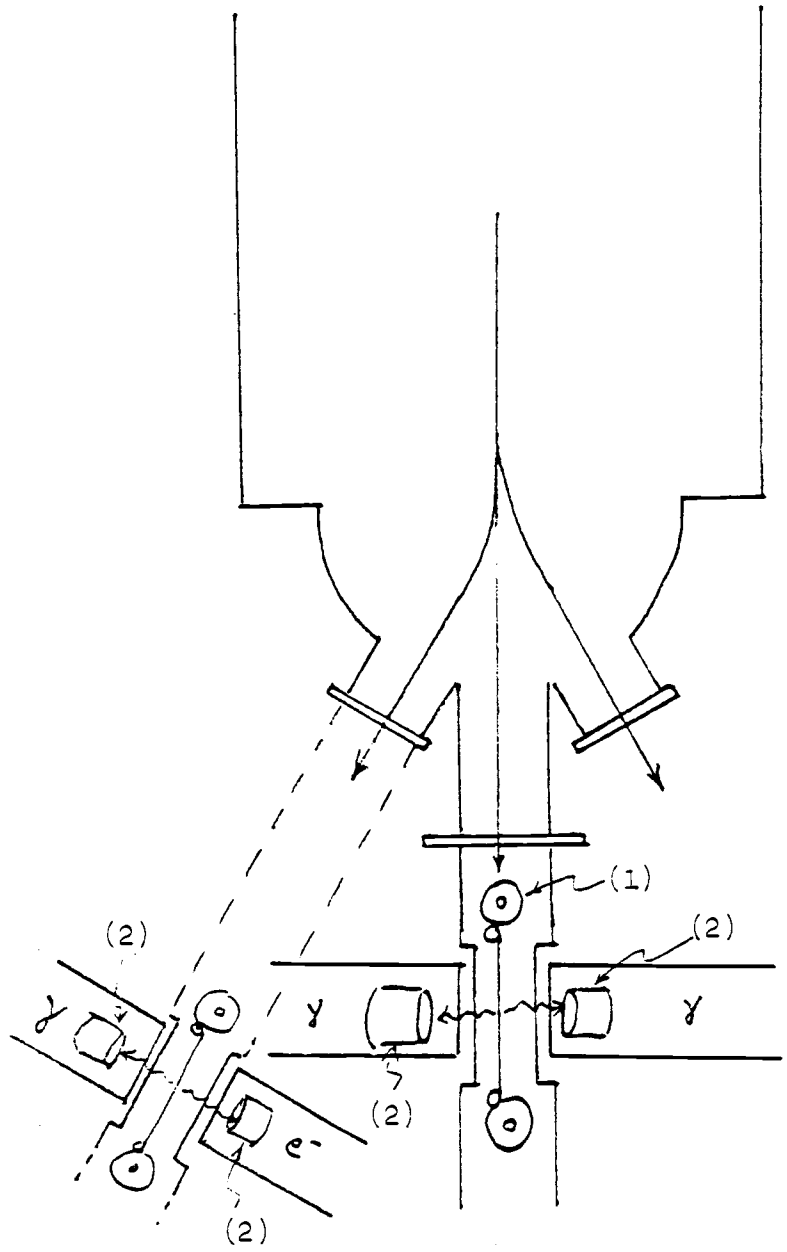

Fig. 13 Experimental setup for γ-ray and conversion electron detection. Only central line is drawn. (1) magnetic tape for isotope depositing and transfering. (2) Ge detector for γ-ray detection or Si(Li) detector for conversion electron detection.

spectrum analyzing program SAMPO on the Ridge computer managed by the nuclear theory group in the Department of Physics, OSU. The possible decays of 15.8h and 1.7h ^{186}Ir were identified. One of the problems in identifying Pt → Ir peaks was that there were always many peaks close together to form a broad peak and it was hard to find their decaying times.

The grand sum data at first went through a primary run of SAMPO and all the peaks were located. In the second run, some modifications were made and the energy and intensity of each peak were calculated. Then every spectrum went through SAMPO to find intensity change of all the peaks in it so that the lifetimes were found for all the single and the double peaks. For a broad peak containing many individual peaks the lifetimes found are not dependable because SAMPO fit differently for different shapes.

By referring the decaying-times and comparing with the coincidence data, we can identify the possible peaks from the Pt to Ir decay.

IV. Summary of results

The experiment results give more information than previous experiments on the ^{186}Pt decay. The single gamma spectrum in Fig. 14 contains all the gamma transitions from the decay chain. The ^{186}Ir gamma transitions are marked with the triangle sign. The 689.5 keV peak is the strongest one and used as the intensity normalization (100). Fig. 15 and Fig. 16 are the coincidence data gated by K_β 100.5, 204.5, 210.3, 256, 280.8, 366.7, 579, 611, 636, 689 keV transitions. The conversion electron spectrum is shown in Fig. 17. From the electron intensities together with the gamma intensities, we can find the conversion coefficients and multipolarities which can help to establish the decay scheme.

Table 1 shows the gamma-ray energies and intensities from ^{186}Pt decay as compared with the previous results [16]. The data are obtained from singles spectra at beam energy 130 Mev and a few of them are only seen from the coincidence spectra. The energy uncertainties are less than 0.1 kev. The coincidence data are shown in table 2.

Table 3 is the internal conversion coefficients of the ^{186}Pt → ^{186}Ir gamma-transitions. The internal electron conversion in heavy nuclei competes with the rela-

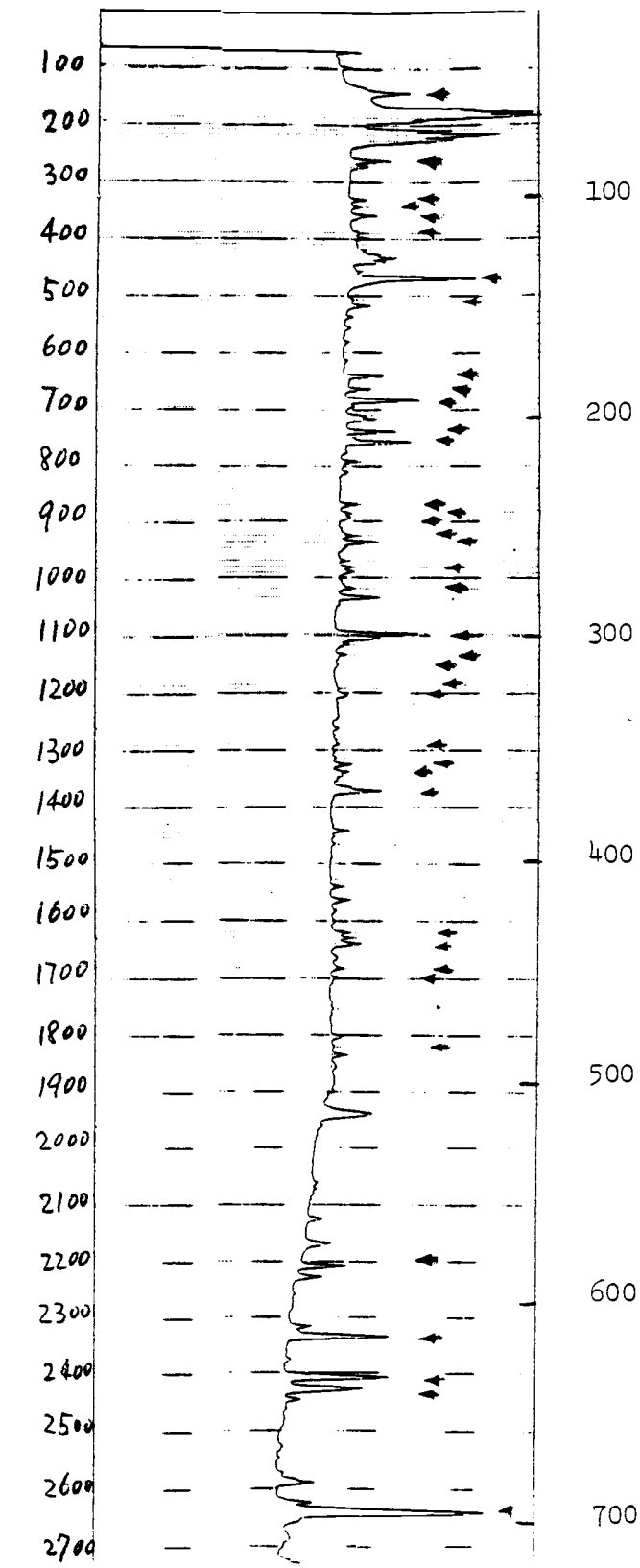

Fig.14 γ-ray spectrum from the $^{14}N(Hf,xn)^{186}Au$ at 130Mev. The spectrum is cut at 700kev to show only the transitions in the ^{186}Pt decay.

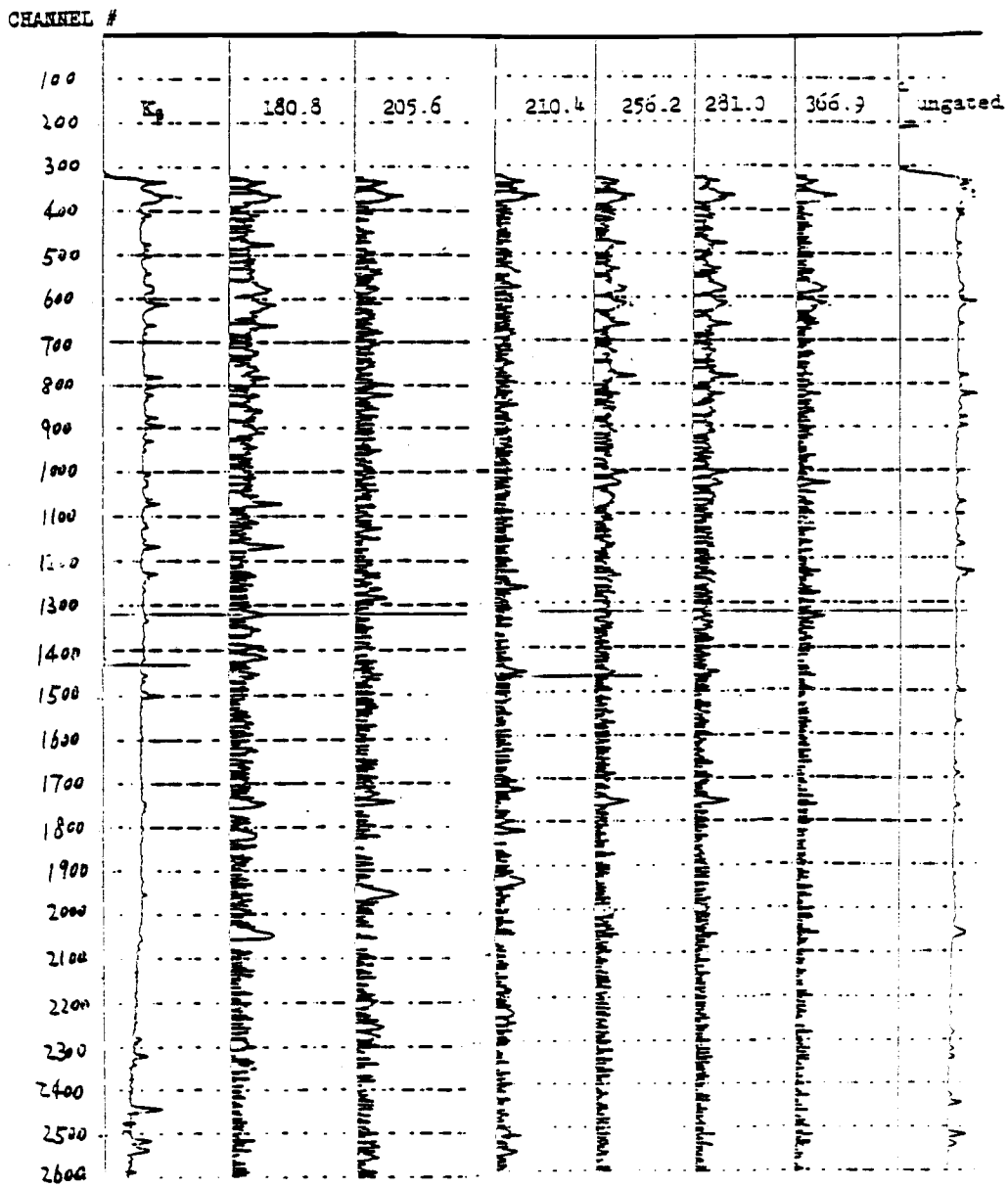

Fig. 15 Coincidence spectra

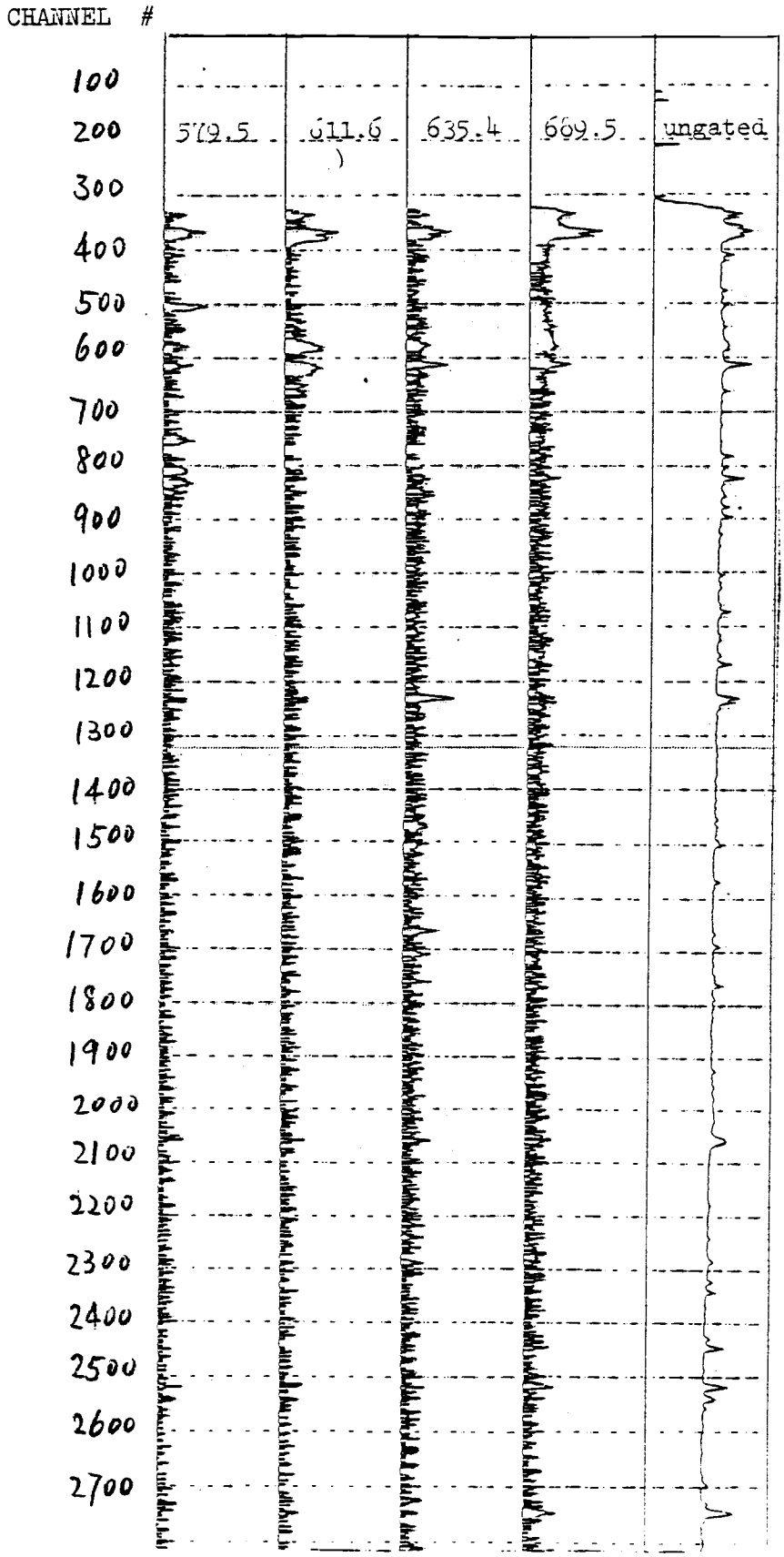

Fig. 16 Coincidence spectra.

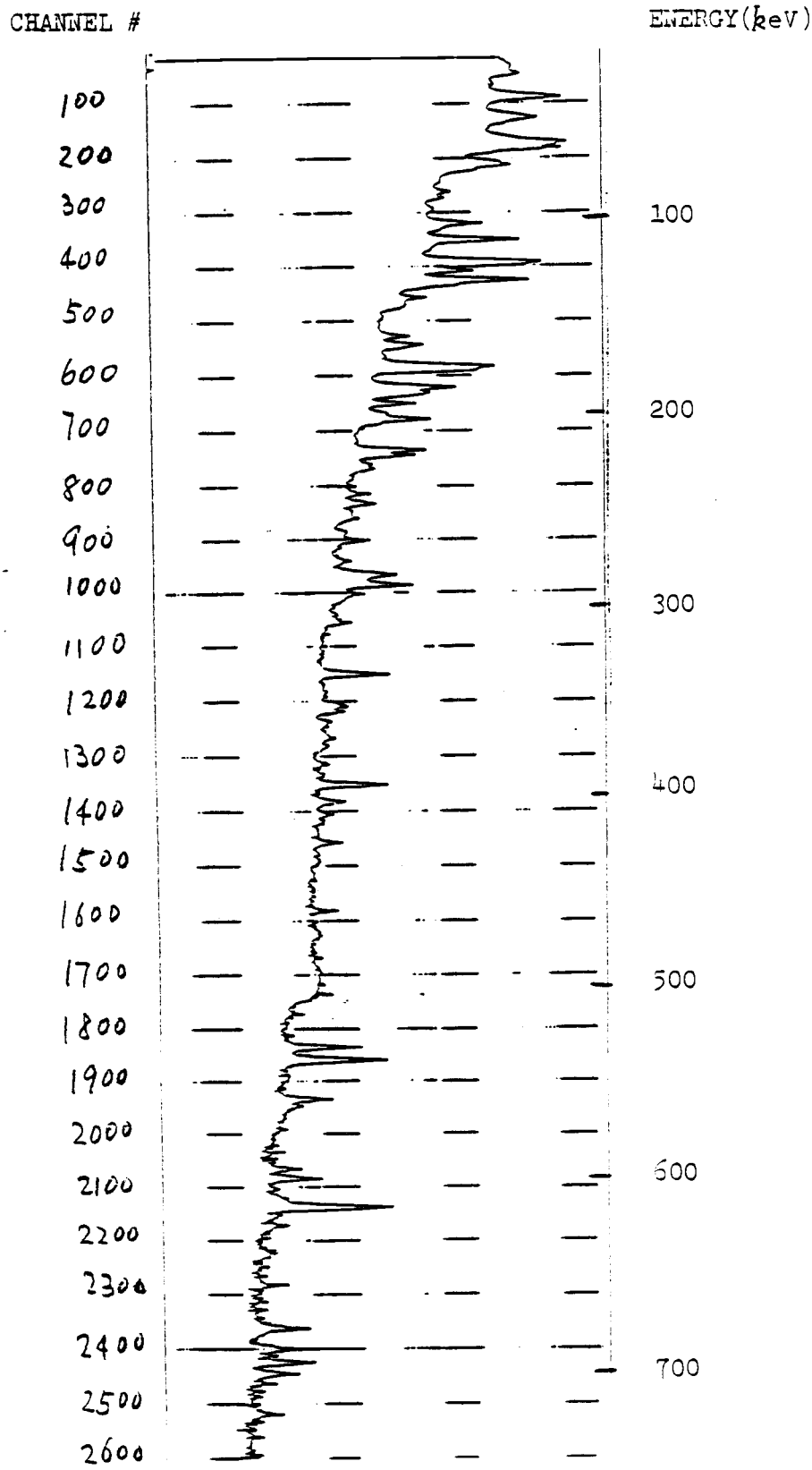

Fig. 17 Conversion electron.

Table 1 Gamma Rays Tentatively Assigned to ^{186}Pt Decay

Present Results		Previous Results	
E_γ(keV)[a]	I_γ	E_γ(keV)	I_γ
54.1	1.28(8)	63	
(84.9)	0.71(2)		
101.9	0.21(1)	101.8(7)	-0.4
104.9	0.10(1)		
109.0	0.40(2)	109.1(4)	0.7(2)
(116.9)	0.12(2)		
149.9	0.43(2)	149.6(4)	0.6(1)
180.8	0.95(5)	180.5(4)	1.7(2)
(186.7)	0.51(2)	186.5(4)	0.8(2)
(194.4)	0.19(2)	194.3(8)	-0.3
205.6	1.62(3)	205.4(3)	2.2(3)
210.4	3.02(5)	210.3(3)	2.6(3)
238.9	0.48(2)	238.7(6)	0.6(3)
242.8	0.31(1)	242.6(12)	0.5(2)
244.8	0.31(3)	244.6(12)	0.4(2)
253.4	0.50(3)	252.8(8)	0.9(2)
256.2	1.57(3)	256.0(4)	2.0(3)
267.5	0.39(1)	267.4(12)	-0.3
269.5	0.47(1)	269.5(10)	0.5(3)
281.0	1.89(4)	280.8(4)	2.4(4)
(299.1)	[b]		
306.2	0.27(2)		
(310.7)	0.12(1)		
(319.8)	0.06(1)		
323.2	0.20(1)	323.6(12)	-0.8
(345.8)	0.15(3)		
355.0	0.56(2)		
358.3	0.46(2)		
365.1	0.58(3)		
366.9	2.43(5)	366.7(4)	3.3(7)
429.9	[b]		
432.2	0.64(3)		
445.6	0.37(2)		
450.0	0.27(1)		
484.6	0.48(2)		
579.5	1.6(1)	579.4(8)	1.7(13)
611.6	6.8(1)	611.5(4)	8.6(8)
635.4	3.1(2)	635.6	$\leq$ 5.4
640.4	0.30(1)		
689.5	100(1)	689.2(3)	100

[a] Energy uncertainties less than 0.1 keV

[b] Seen only in coincidence spectra

Table 2 Coincidence Relationships in the Decay $^{186}Pt \rightarrow {}^{186}Ir$

Gating Transition	Probable Coincidences
180.8	101.9, 149.9, 180.8, 256.2, 281.0, (319.8), (345.8), 355.0, 450.0, (579.5)
205.6	54.1, (186.7), 269.6, 306.2, (310.7), 355.0, 358.3, 429.9, (450.0), 484.6
210.4	54.1, 306.2, 355.0, (450.0)
256.2	101.9, (116.9), 149.9, 180.8, 238.9, 244.8, 253.4, 281.0, (299.1), 355.0, 432.2
281.0	101.9, (116.9), 149.9, 180.8, 238.9, 244.8, 253.4, 256.2, 355.0, 432.2
366.9	244.8, (323.2)
579.5	109.0
611.6	——
635.4	54.1
689.5	——

Table 3 Internal Conversion Coefficients in the Decay $^{186}Pt \rightarrow {}^{186}Ir$

E_γ(keV)	α_K(expt)	α_K(th) E1	M1	E2	Mult.
54.1	3.9(5)[a]	0.35	5.3	63	M1
109.0	0.32(3)	0.26	4.0	0.66	E1
149.9	1.8(2)	0.12	1.7	0.35	M1
180.8	0.85(15)	0.070	1.0	0.21	M1(+E2)
205.6	0.39(4)	0.053	0.66	0.18	M1+E2
210.4	1.0(1)	0.050	0.65	0.17	(M1)
238.9	0.29(2)	0.035	0.44	0.11	M1+E2
267.5	0.82(10)[b]	0.027	0.32	0.078	(M1)
269.6	0.35(5)[b]	0.027	0.32	0.078	M1
281.0	0.21(3)	0.024	0.30	0.070	M1(+E2)
355.0	0.05(1)	0.015	0.15	0.038	E2(+M1)
366.9	0.13(2)	0.014	0.14	0.035	M1
429.9	0.16(3)	0.0096	0.092	0.024	M1
432.2	0.08(1)	0.0096	0.092	0.024	M1
445.5	0.090(15)	0.0088	0.082	0.023	M1(+E2)
450.0	0.090(15)	0.0085	0.080	0.022	M1(+E2)
454.6	0.06(1)	0.0074	0.066	0.019	M1(+E2)
579.5	<0.012	0.0050	0.042	0.013	E1
611.6	0.031(4)	0.0045	0.037	0.011	M1(+E2)
635.4	0.0035(10)[c]	0.0042	0.036	0.010	E1
689.5	≤0.0035	0.0035			E1

[a] Total L-conversion coefficient.

[b] May include 205.6 L-lines.

[c] Corrected for ^{186}Os 636 line.

tively lower gamma-ray transition energies. So the measurement of internal conversion and multipolarities plays an important role in establishing a level scheme.

V. Discussion

It seems not yet possible to establish a complete level scheme for ^{186}Ir low spin states with the information on hand. The strongest 689.5 keV line is almost certainly from 1^+ to 2^- ground state and we need more information to complete the work (Fig. 18). From the coincidence data (table 2) it appears that there is no apparent rotational band. There are some transitions that look like a sequence but have no evidence of where it starts and ends. For example, the 281, 256, 180, 149, 101 transitions in Table 4.

There is a relatively strong E2+M1 line which was not observed in previous experiments with energy 355.0 keV. It may have something to do with the transition between Ir low spin states to high spin states. It is speculated that the 5+ state is the ground state and then there possibly are transitions from low spin excited state to 5+ state. The 434 keV line in Os which is mainly from the 5+ state is observed in the experiment and the intensity as function of time is plotted in Fig. 19. The calculated 5^+ (15.7hr) Ir decay following the 2^- (1.7hr) decay as function of time is plotted in Fig. 20 compared with the decays of 5^+ and 2^- directly following Pt 0^+ ground state decay. We can see that the 5^+ following 2^- decay fits the

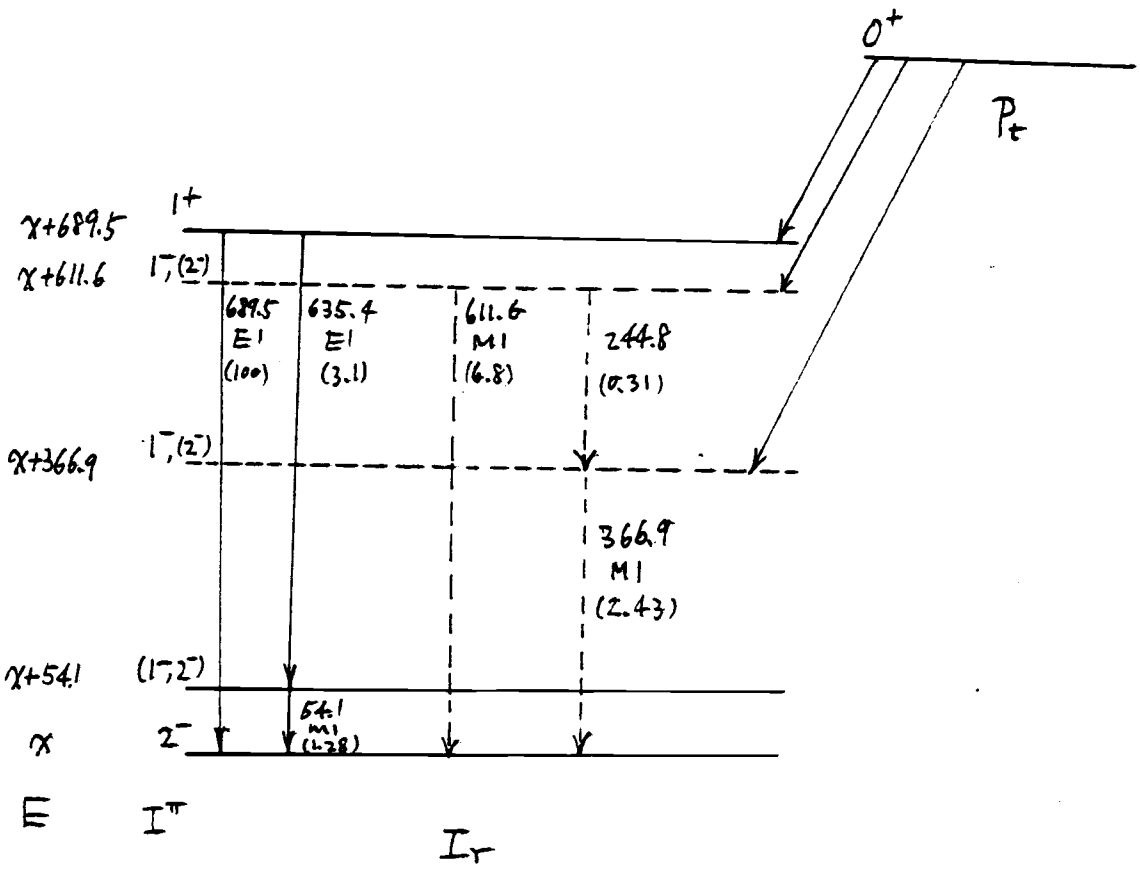

Fig. 18 Some gamma transitions in ^{186}Ir.

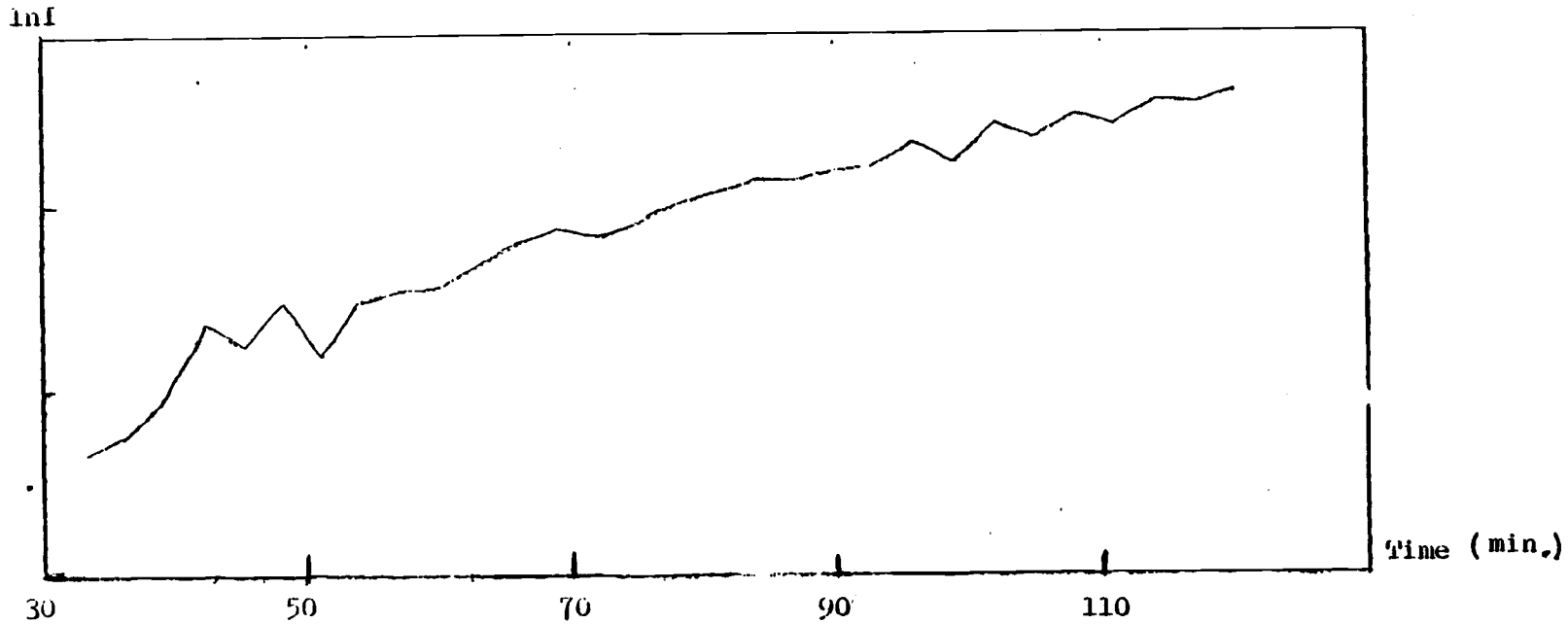

Fig.19 The intensity of 434 kev gamma-ray of 5^+ Ir decay as function of time.

Table 4 Coincidence Data and Their Intensities.

			Coincidence Chains				
mult.	I	I^{TOT}	1	2	3	4	5
M1	1.28(8)	6.3(8)			54.1	54.1	54.1
	0.21(1)		101.9	101.9			
	0.12(2)		(116.9)				
M1	0.43(2)	1.2(1)	149.9	149.9			
M1(+E2)	0.95(5)	1.76(16)	180.8	180.8			
	0.51(2)				(186.7)		
M1+E2	1.62(3)	2.25(8)			205.6		
(M1)	3.02(5)	6.0(3)				210.4	
M1+E2	0.48(2)	0.62(3)	238.9				
	0.31(3)		244.8				
	0.50(3)		253.4				
	1.57(3)		256.2	256.2			
M1	0.47(1)	0.63(2)			269.6		
M1(+E2)	1.89(4)	2.29(7)	281.0	281.0			
			(299.1)				
	0.27(2)				306.2	306.2	
	0.12(1)				(310.7)		
	0.06(1)			(319.8)			
	0.15(3)			(345.8)			
E2(+M1)	0.56(2)	0.59(2)	355.0	355.0	355.0	355.0	
	0.46(2)				358.3		
M1					429.9		
M1	0.64(3)	0.69(3)	432.2				
M1(+E2)	0.27(1)	0.29(1)		450.0	(450.0)	(450.0)	
	0.48(2)				484.6		
E1	1.6(1)	1.6(1)		(579.5)			
E1	3.1(2)	3.1(2)					635.4

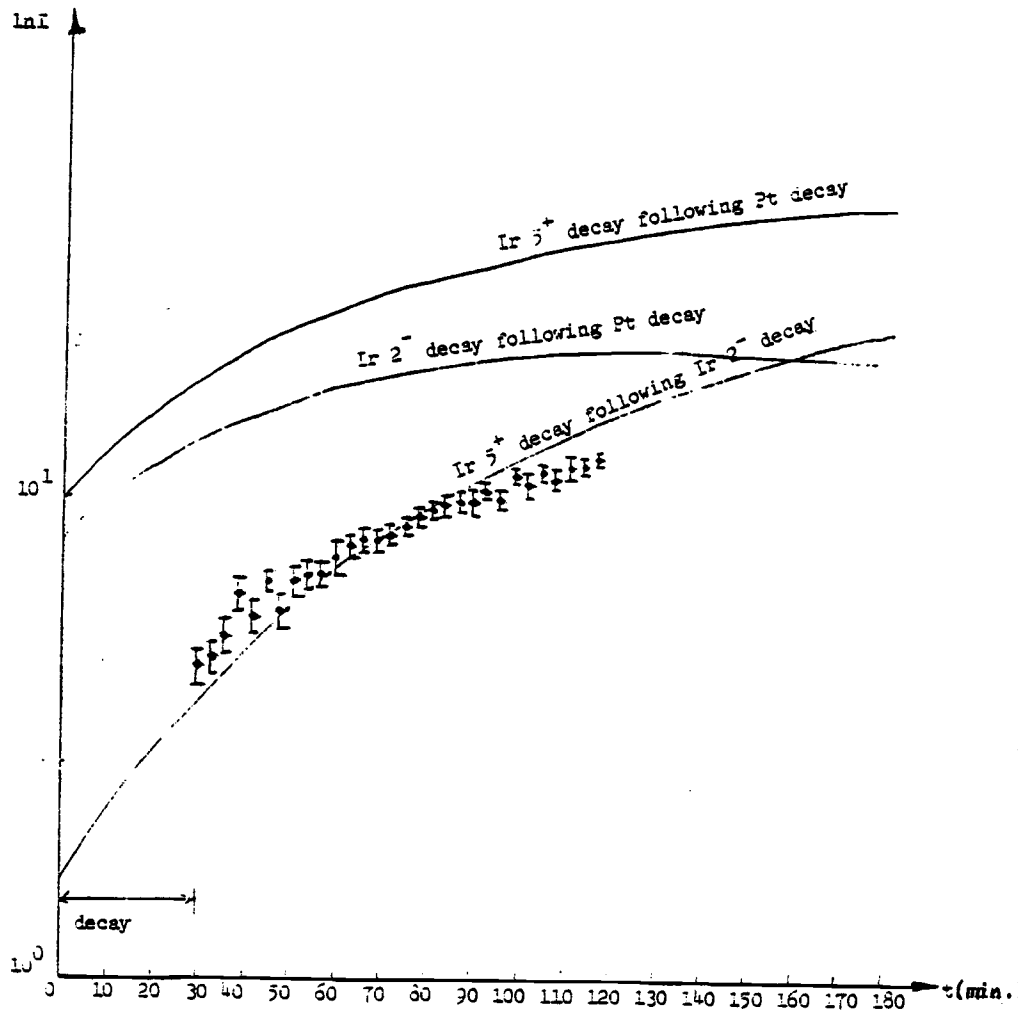

Fig. 20 434 kev rate as compared with theoretical calculations

data better. Considering some mixing of direct 5^+ decay, it will make a good fit. On the other hand, there is no evidence of direct decays from 2^- to 5^+ because in the 2^- isomer decay, the 434 keV line is not observed. [17] The data thus seem contradictory.

In the spectrum there are many peaks together which cannot be resolved so that there may be some more ^{186}Ir transitions that are not identified. The ^{184}Ir data obtained in the same experiment and the information on ^{188}Ir [18] may provide some hints. But the proton Nilsson states are changing very abruptly between atomic number 185 and 187 (Fig. 21). So one expects that there will be a very different level ordering of ^{186}Ir from those of ^{184}Ir and ^{188}Ir.

On the other hand, if we can perform other experiments with less gamma transitions the picture may be clearer. For example, make in-beam measurements for reactions like

$$^{11}B + {}^{178}Hf \rightarrow {}^{186}Ir + 3n$$

or

$$^{4}He + {}^{187}Re \rightarrow {}^{186}Ir + 5n.$$

Or the reaction like

$$^{12}C + {}^{178}Hf \rightarrow {}^{186}Pt + 4n$$

which can eliminate the Au decays may get a better spectrum.

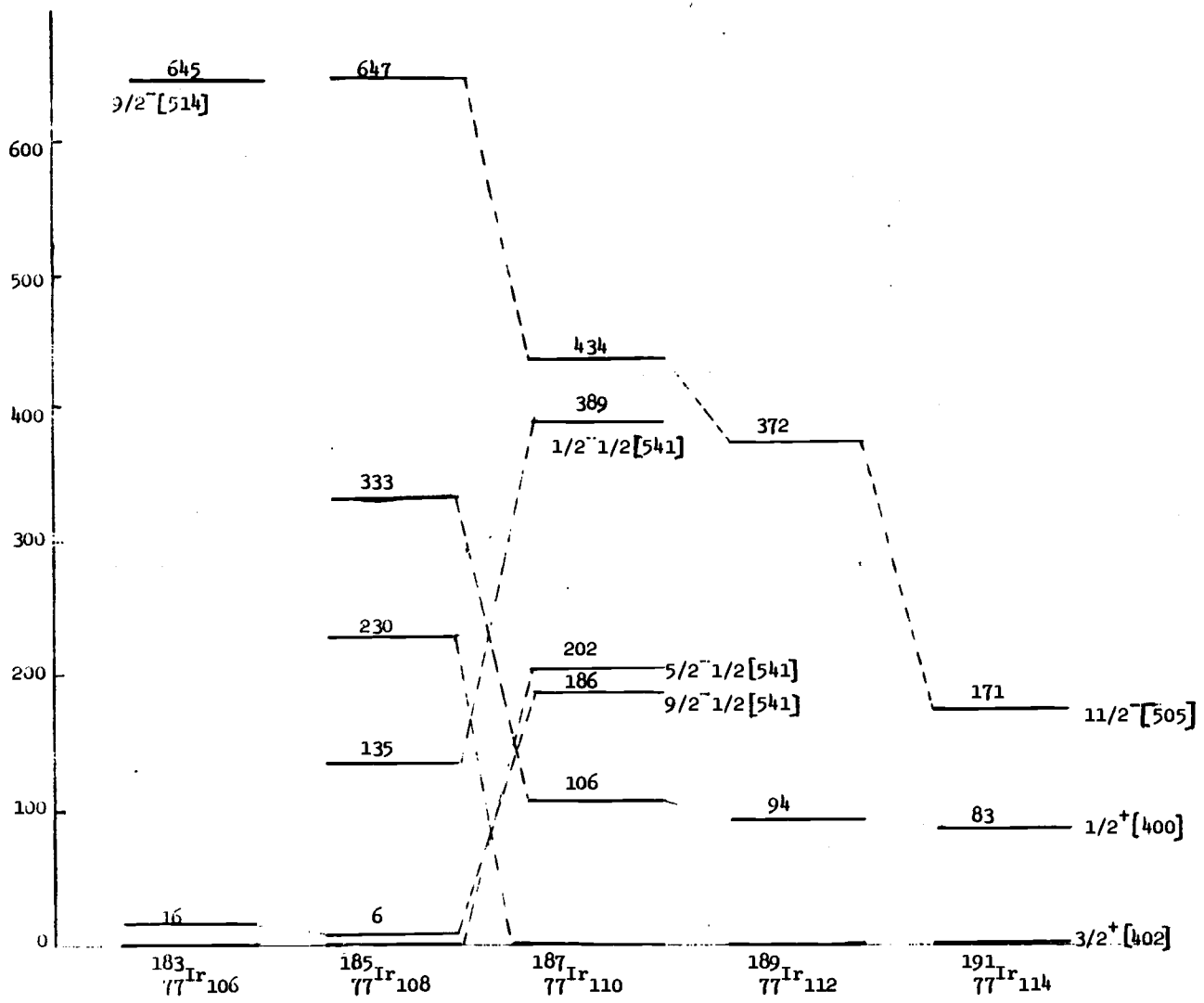

Fig. 21 Proton Nillson states of Ir isotopes.

VI. Conclusion

There is certainly not enough information to establish a level scheme yet. But some new information for ^{186}Ir low spin states is given in the analysis. The 5^+ state may be below the 2^- state and there may be transitions between 5^+ and low spin states. Further investigation is needed to provide more evidence.

REFERENCES

[1] L. W. Nordheim, Phys. Rev. 78, (1950) 294; Rev. Mod. Phys. 23, (1951) 322.

[2] C. J. Gallagher, Jr. and S. A. Moszkowski, Phys. Rev. 111, (1958) 1282.

[3] A. J. Kreiner, D. E. Di Greorio, A. J. Fendrik, J. Davidson and M. Davidson, Nucl. Phys. A432 (1985) 451.

[4] A. J. Kreiner, M. Fenzl, S. Lunardi and M. A. J. Mariscotti, Nucl. Phys. A282 (1977) 243.

[5] A. J. Kreiner, Z. Phys. A288 (1978) 373.

[6] H. Rubinsztein and M. Gustafsson, Phys. Lett. 58B, (1975) 283.

[7] K. J. Hofstetter, T. T. Sugihara, and D. S. Brenner, Phys. Rev. C8 (1973) 2442.

[8] R. Spanhoff, H. Postma and M. J. Canty, Phys. Rev. C18 (1978) 493.

[9] E. Hagn and E. Zech, Z. Physik A297, (1980) 332.

[10] A. L. Allsop, S. Hornung, K. S. Krane and N. J. Stone, J. Phys. G: Nucl. Phys. 8 (1982) 857.

[11] J. P. Davidson, Collective Models of the Nucleus, New York, Academic Press, 1968.

[12] G. T. Emery, R. Hochel, P. J. Daly and K. J. Hofstetter, Nucl. Phys. A211 (1973) 189.

[13] A. J. Kreiner, D. E. Di Greorio, A. J. Fendrik, J. Davidson and M. Davidson, Phys. Rev. C29 (1984) 1572.

[14] F. S. Stephens, Rev. Mod. Phys. Vol. 47, No. 1, (1975) 43.

[15] A. M. Dirac, Principles of Quantum Mechanics, 4th ed., Oxford, Clarendon Press, 1958.

[16] M. Finger et al., CERN report 70-29 (1970), unpublished.

[17] S. W. Yates, J. C. Cunnane and P. J. Daly, Phys. Rev. C11 (1975) 2034.

[18] A. J. Kreiner et al., Nucl. Phys. A425 (1984) 397.

APPENDICES

APPENDIX A

Angular Momentum Commutator in body-fixed frame

The total angular momentum $\vec{I}$ in body-fixed frame as we have seen does not obey the regular commutation rule. We will derive this commutation rule in this appendix. In terms of Euler angles θ_i, express the angular velocity of the body in the body-fixed system:

$$\omega_1 = \dot{\theta}_2 \sin\theta_3 + \dot{\theta}_1 \sin\theta_2 \cos\theta_3$$
$$\omega_2 = \dot{\theta}_2 \cos\theta_3 - \dot{\theta}_1 \sin\theta_2 \sin\theta_3$$
$$\omega_3 = \dot{\theta}_3 - \dot{\theta}_1 \cos\theta_2$$

where θ_i (i=1,2,3) are Euler angles. Let $\overleftrightarrow{T}$ be the moment of inertia tensor: then the angular momentum of the body is

$$\vec{I} = \overleftrightarrow{T} \cdot \vec{\omega}$$

We express I_i in terms of the Euler angles and their conjugate momenta P_{θ_i} in order to evaluate the commutator. The Lagrangian L for a rotating rigid body is

$$\mathcal{L} = \frac{1}{2} \vec{\omega} \cdot \overleftrightarrow{T} \cdot \vec{\omega}$$

and following this we get the conjugate momenta of θ_i's as

$$P_{\theta_i} = \frac{\partial \mathcal{L}}{\partial \dot{\theta}_i}$$

By solving for the angular momenta we get

$$I_1 = P_{\theta_2} \sin\theta_3 + (P_{\theta_1} - P_{\theta_3} \cos\theta_2) \cos\theta_3 / \sin\theta_2$$
$$I_2 = P_{\theta_2} \cos\theta_3 - (P_{\theta_1} - P_{\theta_3} \cos\theta_2) \sin\theta_3 / \sin\theta_2$$
$$I_3 = P_{\theta_3} .$$

The only thing necessary to calculate the angular momentum commutator is to work out the commutators of the form $[P_i, \cos\theta_i]$ by using the quantum condition relating the classical Poisson bracket with the commutator [15]. Then we get

$$[I_1, I_2] = -i\hbar I_3 \qquad \text{cyclically.}$$

The angular momenta of the odd nucleons in the body-fixed system are not good quantum numbers and they obey the normal angular momentum commutation rule.

APPENDIX B

Symmetrization of State Function $|EIMK\rangle$

If the deformed nucleus has axial symmetry there will be no difference between $K=\Omega$ and $K=-\Omega$. We have to symmetrize the state function to get the energy degeneracy. It has been shown that th state function can be written as a product of a rotational function $|EIMK\rangle$ and a particle function $|\Omega\rangle$:

$$|EIMK=\Omega\rangle = |EIMK\rangle\,|\Omega\rangle$$

where $|EIMK\rangle$ is the eigenfunction of operators $\vec{I}$ and $\vec{K}$.

For example, the rotational transformation between laboratory and body-fixed frames is made by the rotation matrices D^{I}_{MK}. These D's are the $(2I+1)$ dimensional representation of the rotation group R(3) i.e.

$$|I,K\rangle^{B} = \sum_{M} D^{I}_{M,K}(\theta_i)\,|I,M\rangle^{L};$$

with Euler angles θ_i $(i=1,2,3)$. Obviously, these functions $D^{I}_{MK}(\theta_i)$ are simultaneous eigenfunctions of the square of the total angular momentum $\vec{I}^2$, the projection of the angular momentum on the Z-axis I_Z and on the 3-axis I_3, with eigenvalues $I(I+1)$, M and K. So, we will take D^{I}_{MK} as our rotational function $|EIMK\rangle$.

$$|EIMK\rangle \sim D^{I}_{M,K} \ .$$

The particle function $|\Omega\rangle$ can be constructed by the angular momentum eigenfunctions $|j\Omega\rangle$,

$$|\Omega\rangle = \sum_{j} C_{j\Omega} |j\Omega\rangle ,$$

then

$$|EIMK=\Omega\rangle = \frac{1}{\sqrt{2}} \sum_{j} C_{j\Omega} \left[D^{I}_{M,K}(\theta_i) |j,K\rangle + (-1)^{I-j} D^{I}_{M,-K}(\theta_i) |j,-K\rangle \right].$$

Now we are in the position of evaluating the matrix elements of H_c.